Electronic Supplementary Information

Novel primary phosphinecarboxamides derived from diamines

Erica N. Faria, Andrew R. Jupp, Jose M. Goicoechea*

Department of Chemistry, University of Oxford

Chemistry Research Laboratory, 12 Mansfield Road, OX1 3TA, Oxford, United Kingdom

Email: jose.goicoechea@chem.ox.ac.uk

Contents:

1. Experimental details

2. Single crystal X-ray diffraction data

3. Computational details

4. References

1. Experimental details

1.1 General experimental details

All reactions and product manipulations were carried out under an inert atmosphere of argon using standard Schlenk-line or glovebox techniques (MBraun UNIlab glovebox maintained at < 0.1 ppm H_2O and < 0.1 ppm O_2) unless otherwise noted. [Na(dioxane)$_x$][PCO] was synthesized according to literature procedures and stored at ambient temperature in an inert atmosphere glovebox.[1] The suppliers and purification procedures for commercially available chemicals are detailed in Table S1.

Table S1: Supplier and purification procedures for commercially available chemicals.

Reagent	Supplier	Purity	Purification
$H_2NNH_2 \cdot HCl$	Sigma Aldrich	97%	Used as received
$H_2N(CH_2)_2NH_2$	Aldrich	99%	Refluxed over Na, distilled
HCl (aq. soln.)	Fisher	S.G. 1.18 (37%)	Used as received
18-crown-6	Alfa Aesar	99%	Distilled under vacuum with heating
KHMDS	Sigma Aldrich	95%	Used as received
MeI	Sigma Aldrich	99.5%	Used as received

Tetrahydrofuran (THF; Sigma Aldrich, 99.9%) was distilled from a sodium/benzophenone mixture. Pyridine (py; Alfa Aesar, 99+%) was distilled over CaH_2. Hexane (Sigma Aldrich, HPLC grade), and toluene (Sigma Aldrich, HPLC grade) were purified using an MBraun SPS-800 solvent system. d_8-THF (Fluorochem, >99.5%) and d_5-pyridine (d_5-py; Cambridge Isotope Laboratories Inc, 99.5%) were dried over CaH_2, vacuum distilled, and degassed before use. All solvents were stored under argon in gas-tight ampoules over activated 3 Å molecular sieves

and degassed before use. Deionised water was obtained from a Millipore Milli-Q purification system and sparged overnight with nitrogen.

NMR spectroscopy: NMR samples were prepared inside an inert atmosphere glovebox in NMR tubes fitted with a gas-tight valve. ^{1}H NMR spectra were recorded at either 499.9 MHz or 400.1 MHz on a Bruker AVIII 500 or a Bruker AVIII 400 NMR spectrometer, respectively. ^{13}C{^{1}H} NMR spectra were recorded at either 125.8 MHz or 100.6 MHz on a Bruker AVII 500 fitted with a cryoprobe or a Bruker AVIII 400 NMR spectrometer, respectively. ^{31}P NMR spectra were recorded on 202.4 MHz or 162.0 MHz on a Bruker AVIII 500 or a Bruker AVIII 400 NMR spectrometer, respectively. ^{1}H and ^{13}C NMR spectra are reported relative to tetramethylsilane (TMS) and referenced to the most downfield residual solvent resonance where possible (d_5-pyridine: δ_H = 8.74 ppm, δ_C = 150.35 ppm; d_8-THF: δ_H = 3.58 ppm, δ_C = 67.57 ppm). ^{31}P NMR spectra were externally referenced to an 85% solution of H_3PO_4 in H_2O (δ = 0 ppm). Data analysis was performed using Bruker TopSpin 4.0.7 software.

Elemental analysis: CHN elemental microanalyses were carried out by Elemental Microanalysis Ltd., Devon. Samples were submitted in Pyrex ampoules sealed under vacuum. All values are given as percentages.

1.2 Synthesis of compounds

$\underline{H_2NNHC(O)PH_2}$ (**1**)

[Na(dioxane)$_{1.97}$][PCO] (931.8 mg, 3.65 mmol) and H_2NNH_2·HCl (250 mg, 3.65 mmol) were weighed into a Schlenk tube. THF (20 mL) was added to the solids and the resulting mixture was stirred overnight. On the following day, the pale-yellow solution was filtered into a pre-weighed Schlenk and the solid was washed once with THF (20 mL) and filtered again. The

two fractions were combined and the solvent evaporated at 0˚C under dynamic vacuum to yield the product as an oil (118.1 mg, 35% yield). Single crystals of **1a** and **1b**·(18-crown-6)$_{0.5}$ were obtained by cooling a toluene solution of **1** to −35˚C, and by layering a THF solution of **1** and one equivalent of 18-crown-6 with hexane, respectively.

¹H NMR (500.3 MHz, d_5-pyridine): δ (ppm) 10.73 (s br, 2H; NH (**1a**)), 10.20 (s br, 1H; NH (**1b**)), 5.42 (s br, 2H; NH_2 (**1b**)), 5.18 (s br, 4H; NH_2 (**1a**)), 4.02 (d, 2H, $^1J_{H–P}$ = 218 Hz; PH_2 (**1b**)), 3.72 (d, 4H, $^1J_{H–P}$ = 206 Hz; PH_2 (**1a**)).

¹H{³¹P} NMR (400.2 MHz, d_5-pyridine): δ (ppm) 4.02 (s, 2H, PH_2 (**1b**)), 3.72 (s, 4H, PH_2 (**1a**)); other resonances unchanged from ¹H NMR spectrum.

³¹P NMR (162.0 MHz, d_5-pyridine): δ (ppm) −139.9 (t, $^1J_{P–H}$ = 206 Hz; (**1a**)), −128.2 (td, $^1J_{P–H}$ = 218 Hz, $^3J_{P–H}$ = 4.6 Hz (**1b**)).

³¹P{¹H} NMR (162.0 MHz, d_5-pyridine): δ (ppm) −139.9 (s, **1a**), −128.2 (s, **1b**).

¹³C{¹H} NMR (125.8 MHz, d_5-pyridine): δ (ppm) 172.56 (d, $^1J_{C–P}$ = 9 Hz; PC(O), (**1a**), 181.51 (s, PC(O), (**1b**)).
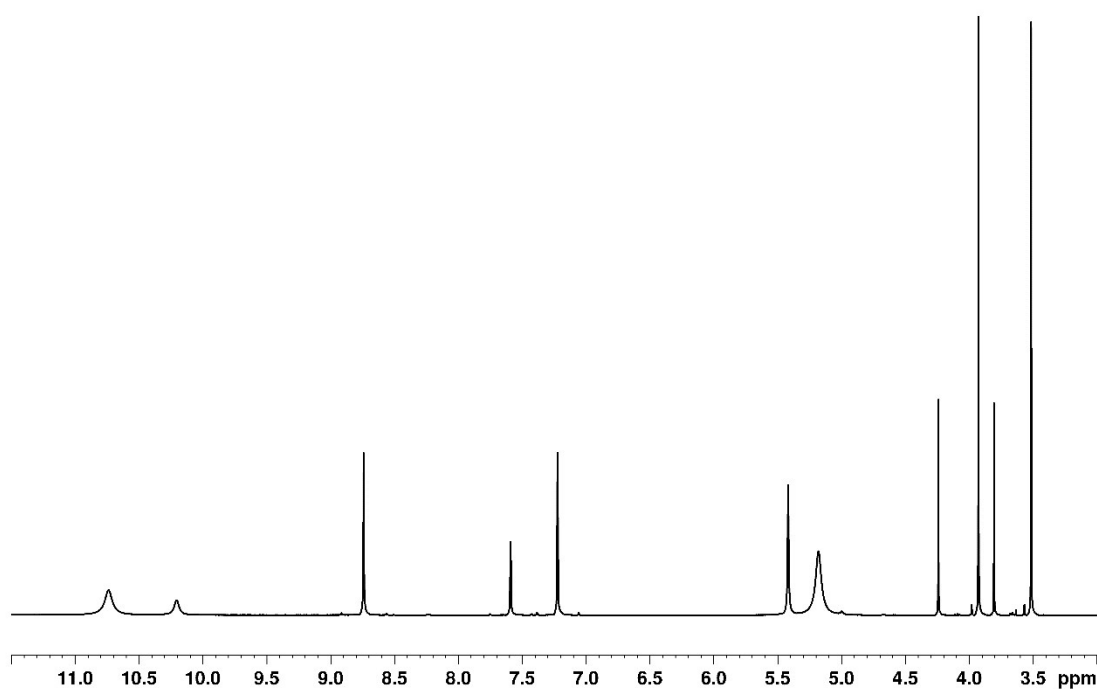
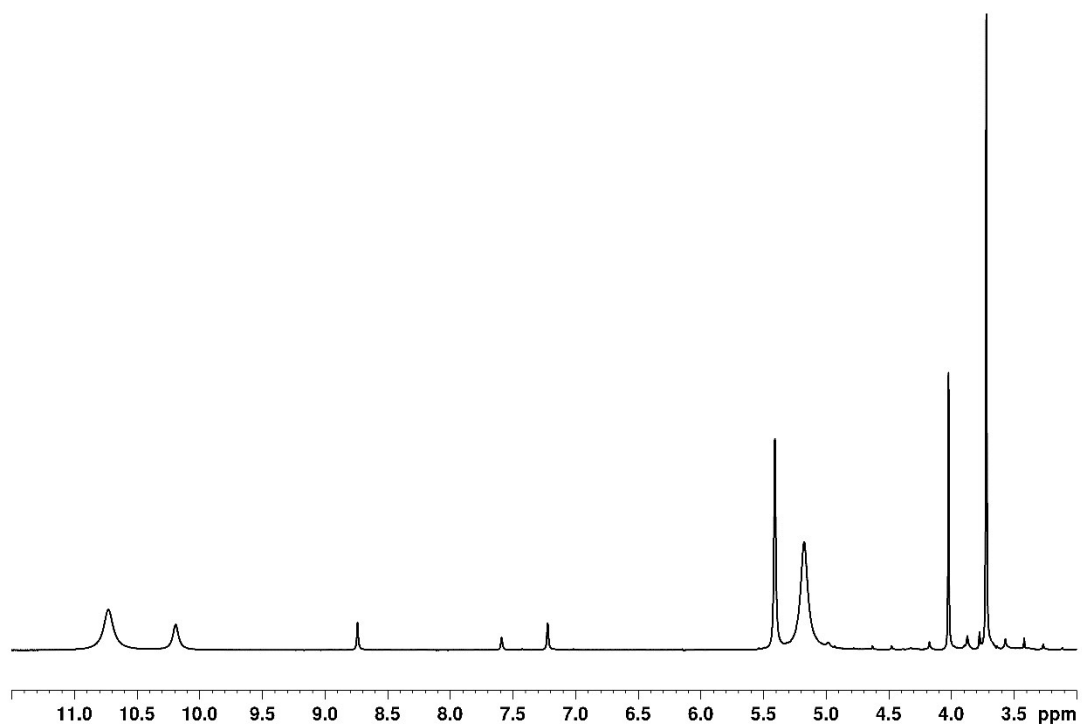**Figure S1:** ^{1}H NMR spectrum of a d_5-pyridine solution of **1**.

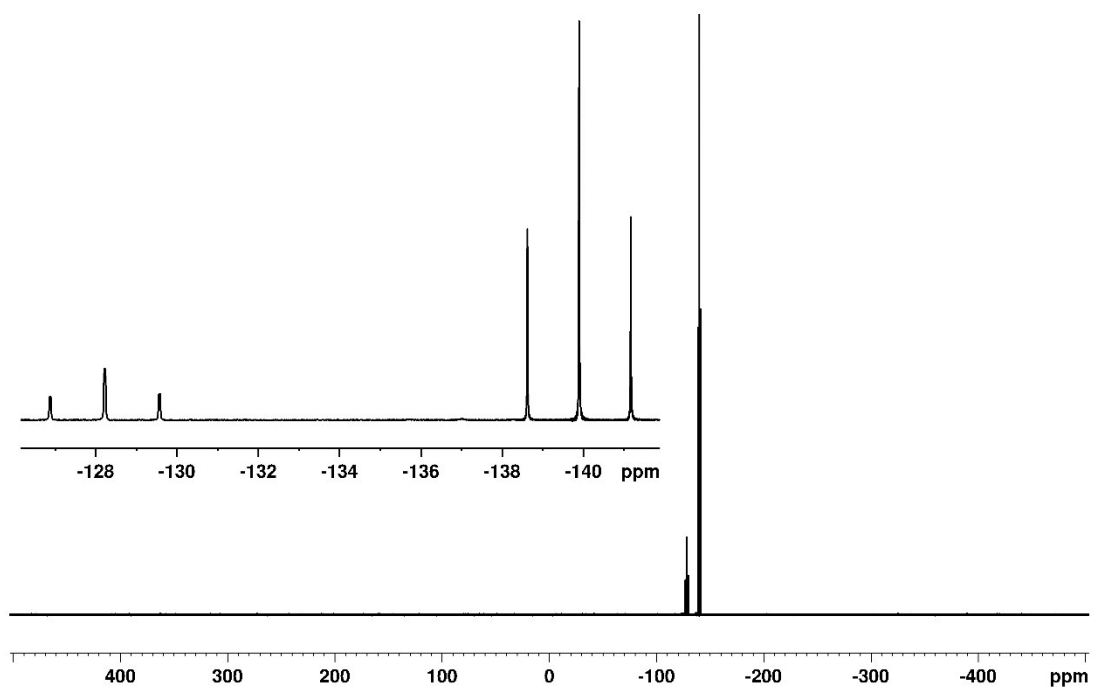**Figure S2:** ^{1}H{^{31}P} NMR spectrum of a d_5-pyridine solution of **1**.

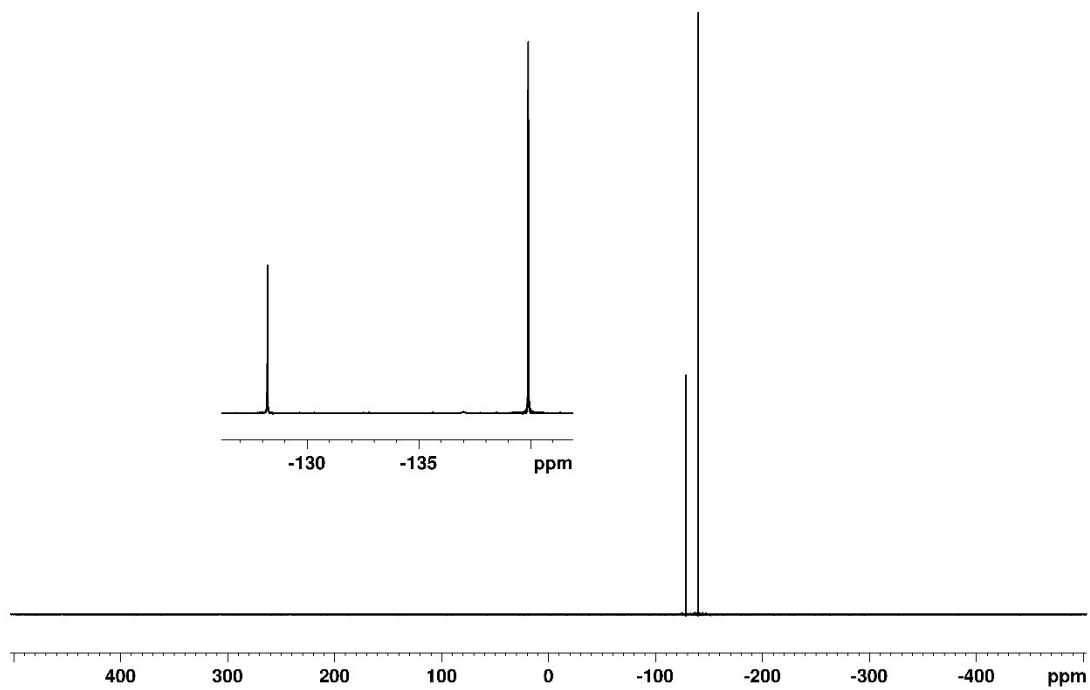**Figure S3:** ^{31}P NMR spectrum of a d_5-pyridine solution of **1**.

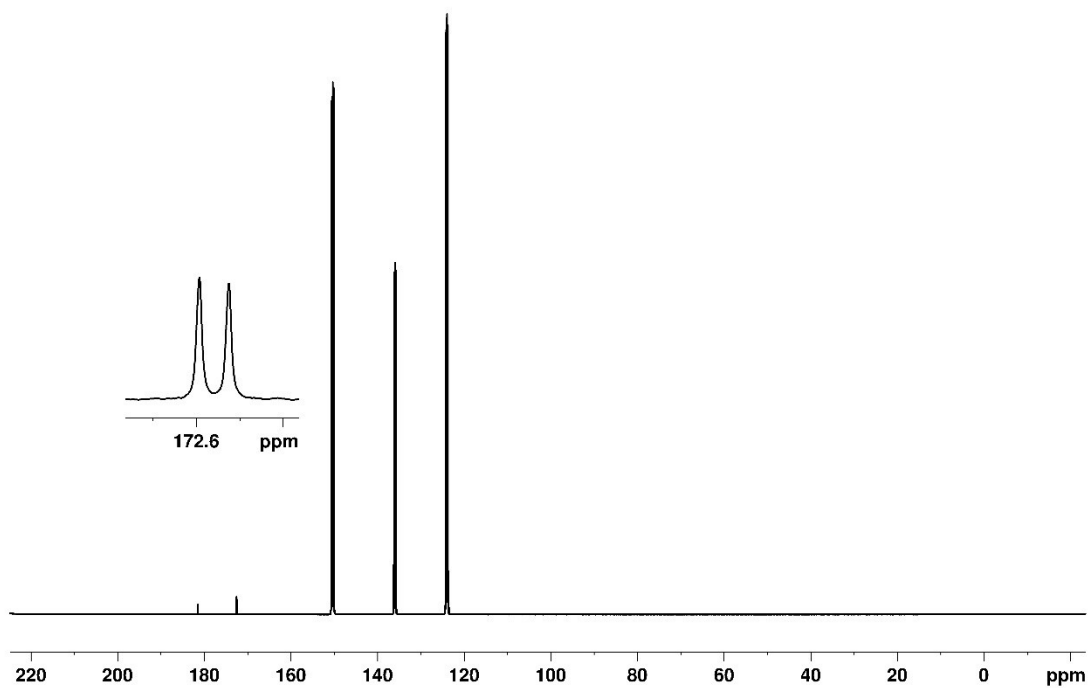**Figure S4:** $^{31}P\{^1H\}$ NMR spectrum of a d_5-pyridine solution of **1**.

Figure S5: $^{13}C\{^1H\}$ NMR spectrum of a d_5-pyridine solution of **1**.

PH$_2$C(O)NH(CH$_2$)$_2$NHC(O)PH$_2$ (**2**)

[Na(dioxane)$_{2.08}$][PCO] (11.3 g, 42.6 mmol) and H$_2$N(CH$_2$)$_2$NH$_2$·2HCl (2.83 g, 21.3 mmol) were weighed into a Schlenk tube. Distilled water (50 mL) was added to the solids resulting in a pale-yellow solution with light brown precipitate (the solid became pale yellow after stirring for 10 minutes). The mixture was stirred overnight. The pale-yellow solution was filtered and the solvent evaporated. The product was extracted into THF (3 × 15 mL). Volatiles were removed at 0˚C under dynamic vacuum to yield the product as a white solid (854.2 mg, 22% yield). Single crystals of **2** were obtained by slow diffusion of hexane into a pyridine solution of **2**.

^{1}H NMR (499.9 MHz, d_5-pyridine): δ (ppm) 9.53 (s br, 2H; N*H*), 3.72 (d, 4H, $^1J_{H–P}$ = 208 Hz; P*H$_2$*), 3.68 (m; C*H$_2$*).

^{1}H{^{31}P} NMR (499.9 MHz, d_5-pyridine): δ (ppm) 3.72 (s, 4H, P*H$_2$*); other resonances unchanged from ^{1}H NMR spectrum.

^{31}P NMR (202.3 MHz, d_5-pyridine): δ (ppm) −132.99 (t, $^1J_{P–H}$ = 208 Hz).

^{31}P{^{1}H} NMR (202.3 MHz, d_5-pyridine): δ (ppm) −132.99 (s).

^{13}C{^{1}H} NMR (125.7 MHz, d_5-pyridine): δ (ppm) 173.52 (d, $^1J_{C–P}$ = 7 Hz; P*C*(O)), 40.77 (s; *C*H$_2$).

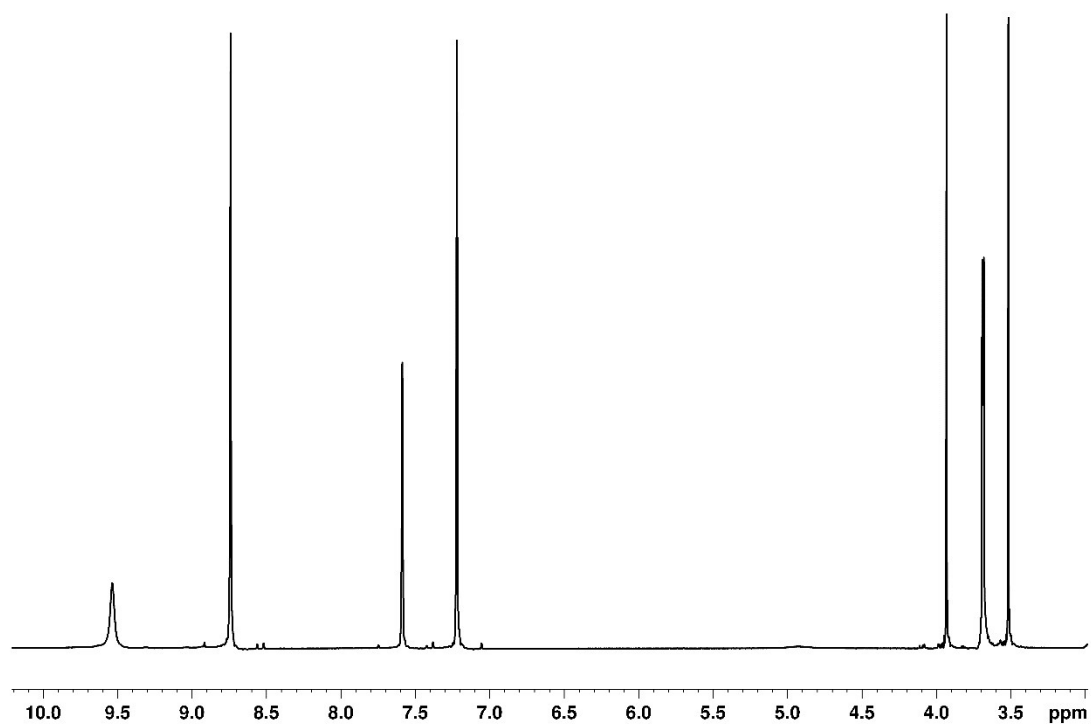**CHN** Calcd. (Found) for C$_4$H$_{10}$N$_2$O$_2$P$_2$: 26.68 (26.92), 5.60 (5.56), 15.56 (15.35).

Figure S6: ^1H NMR spectrum of a d_5-pyridine solution of **2**.

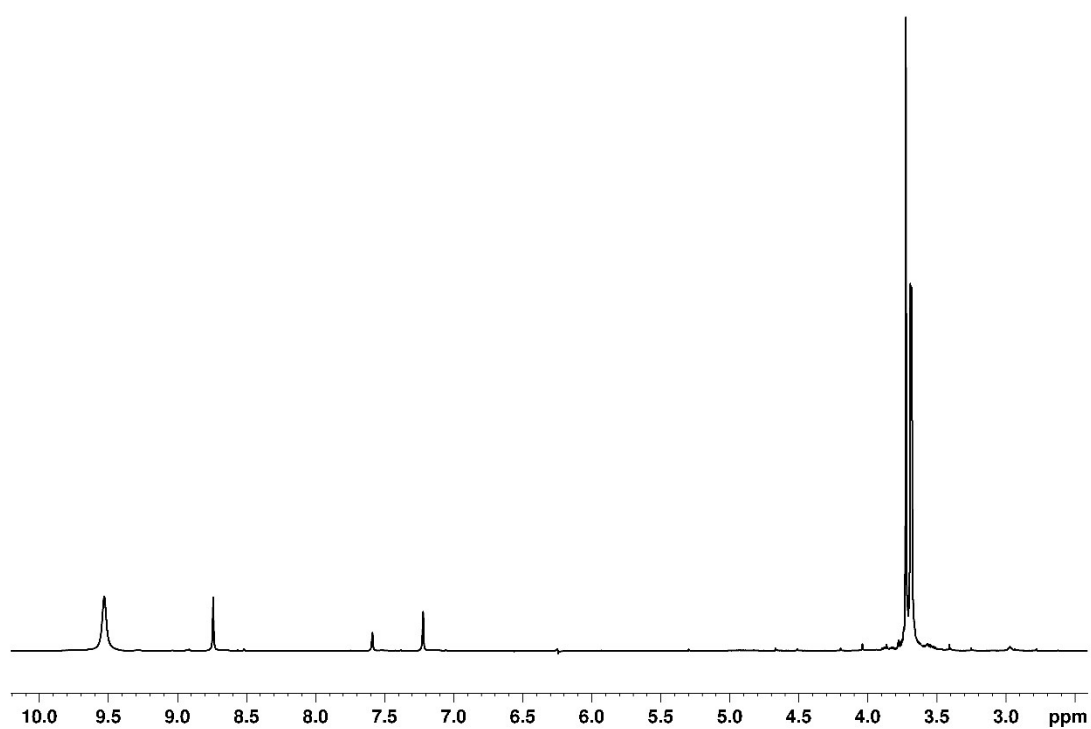**Figure S7:** $^1H\{^{31}P\}$ NMR spectrum of a d_5-pyridine solution of **2**.
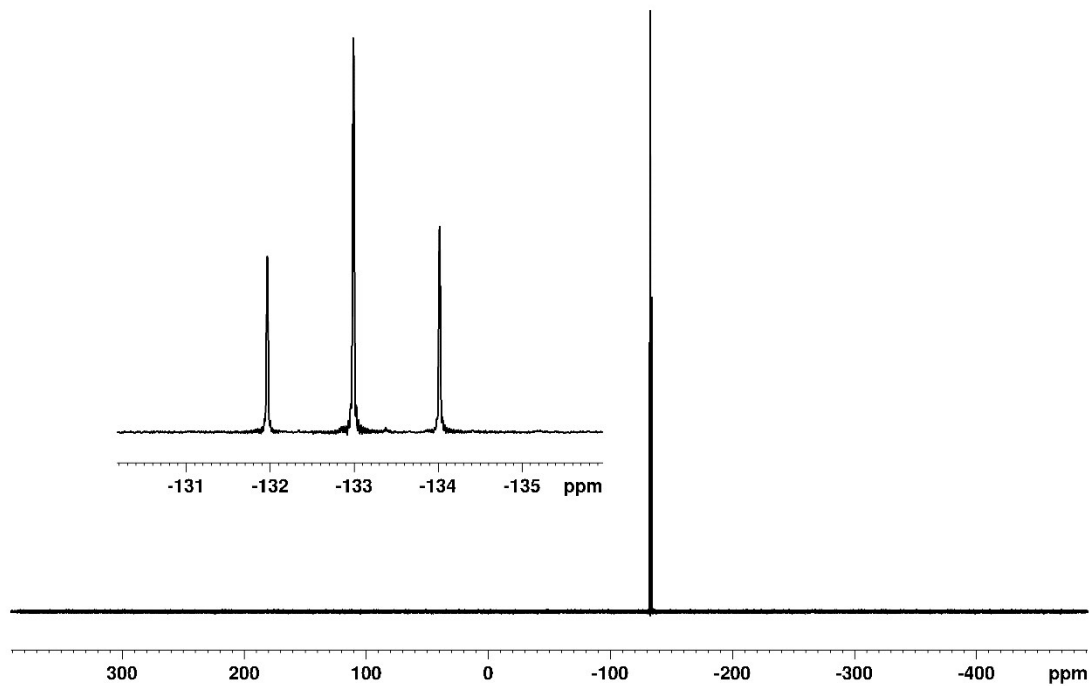
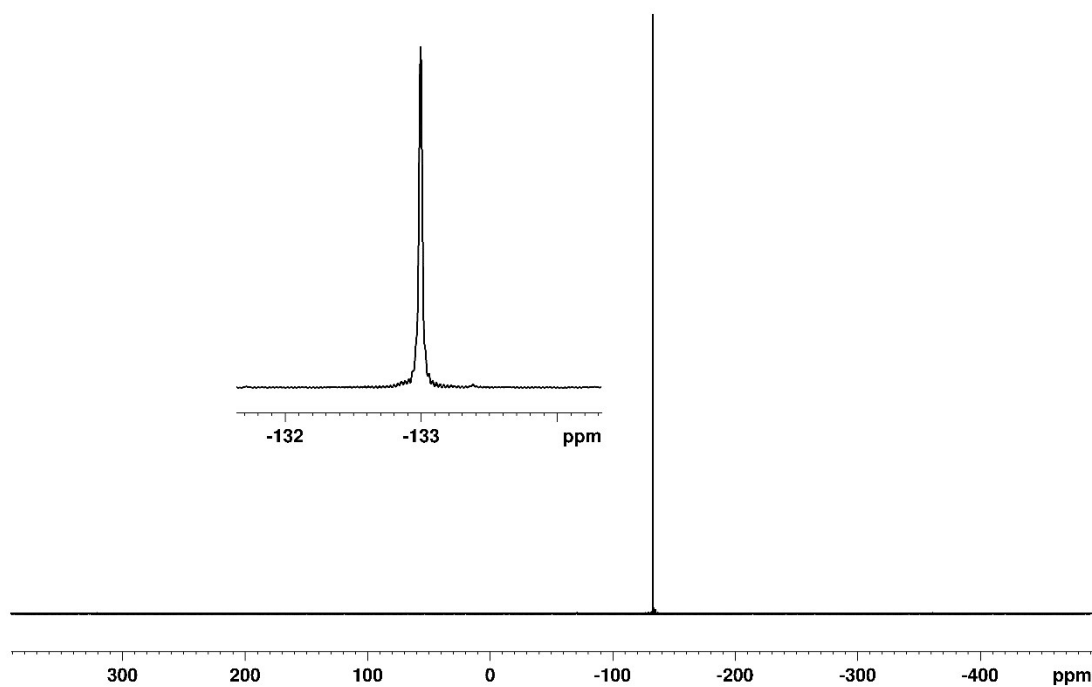**Figure S8:** ^{31}P NMR spectrum of a d_5-pyridine solution of **2**.

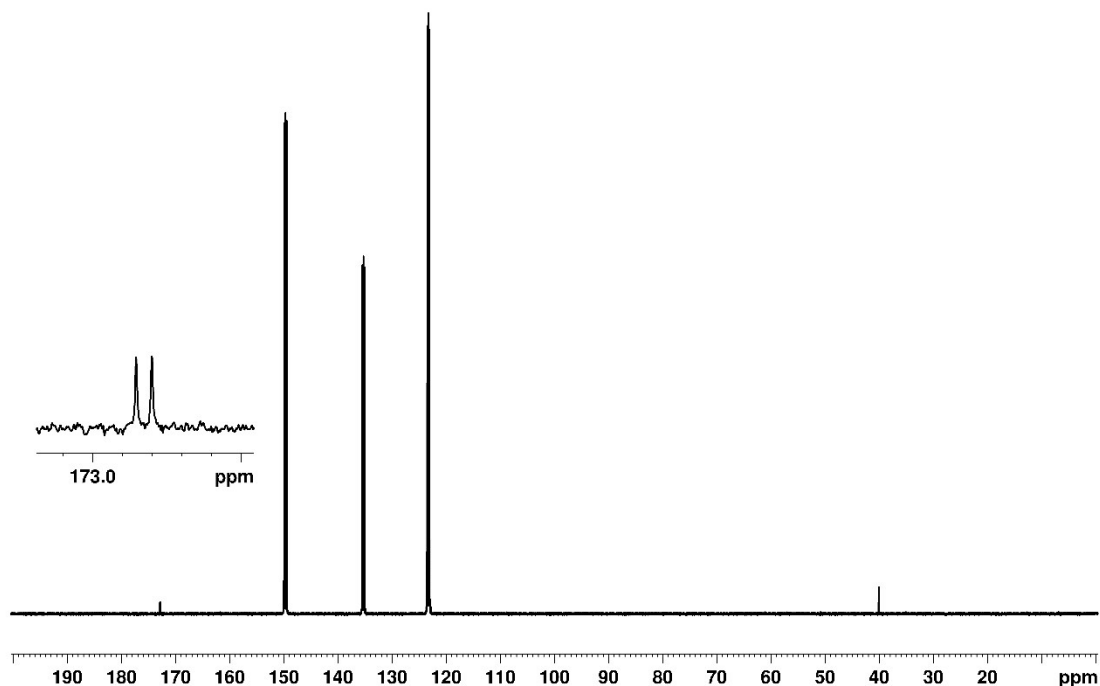**Figure S9:** ^{31}P NMR spectrum of a d_5-pyridine solution of **2**.

Figure S10: $^{13}C\{^1H\}$ NMR spectrum of a d_5-pyridine solution of **2**.

[K(18-crown-6)][**3**]

[Na(dioxane)$_{1.97}$][PCO] (559.1 mg, 2.19 mmol) and H$_2$NNH$_2$·HCl (150 mg, 2.19 mmol) were weighed into a Schlenk tube. THF (15 mL) was added to the solids and the resulting mixture was stirred overnight. On the next day, the pale-yellow solution was filtered into a pre-weighed Schlenk and the solid was washed once with THF (10 mL) and filtered again. The two fractions were combined. Benzyl potassium (285.1 mg, 2.19 mmol) and 18-crown-6 (578.7 mg, 2.19 mmol) were weighed in another Schlenk and dissolved in THF (15mL). The benzyl potassium/18-crown-6 mixture was added to **1** and stirred for 15 minutes. The solution was kept in the freezer for a day to yield colourless crystals that were filtered and isolated (117.2 mg, 15% crystalline yield). Single crystals of [K(18-crown-6)][*cis-cis-***3a**] were obtained by slow diffusion of hexane into a pyridine solution of [K(18-crown-6)][**3**]. We were unable to obtain a suitable elemental analysis for this sample due to its instability.

¹H NMR (499.9 MHz, d_5-pyridine): δ (ppm) 7.10 (br s; N*H* (***trans-cis*-3a**)), 5.27 (br s; N*H₂* (***trans*-3c**)), 4.49 (br s; N*H₂* (***trans-cis*-3a**)), 4.08 (d, $^1J_{P-H}$ = 190 Hz; P*H₂* (***trans*-3c**), 3.68 (m; residual THF), 3.51 (s; 18-crown-6), 2.95 (d, $^1J_{P-H}$ = 150 Hz; P*H* (***trans-cis*-3a**)), 1.63 (m; residual THF).

¹H{³¹P} NMR (499.9 MHz, d_5-pyridine): δ (ppm) 4.08 (s; P*H₂* (***trans*-3c**)), 2.95 (s; P*H* (***trans-cis*-3a**); other resonances unchanged from ¹H NMR spectrum.

³¹P NMR (162.0 MHz, d_5-pyridine): δ (ppm) −128.6 (t, $^1J_{P-H}$ = 190 Hz; ***trans*-3c**), −109.4 (br d, $^1J_{P-H}$ = 150 Hz, ***trans-cis*-3a**).

³¹P{¹H} NMR (162.0 MHz, d_5-pyridine): δ (ppm) −128.6 (s, ***trans*-3c**), −109.4 (br s, ***trans-cis*-3a**).

¹³C{¹H} NMR (125.8 MHz, d_5-pyridine): δ (ppm) 207.90 (d, $^1J_{C-P}$ = 62 Hz; P*C*(O), ***trans-cis*-3a**), 162.43 (d, $^1J_{C-P}$ = 24 Hz; P*C*(O), ***trans*-3c**), 70.78 (s, 18-crown-6), 68.29 (bs, residual THF), 26.27 (bs, residual THF).
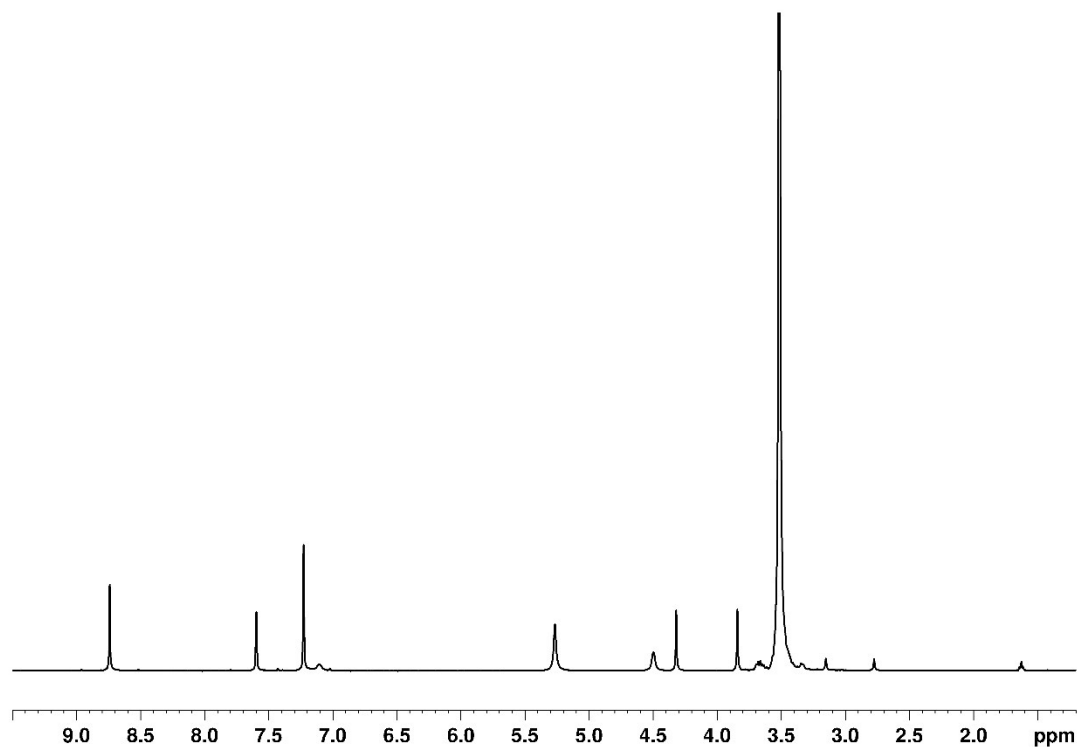
Figure S11: ^{1}H NMR spectrum of a d_5-pyridine solution of [K(18-crown-6)][**3**].
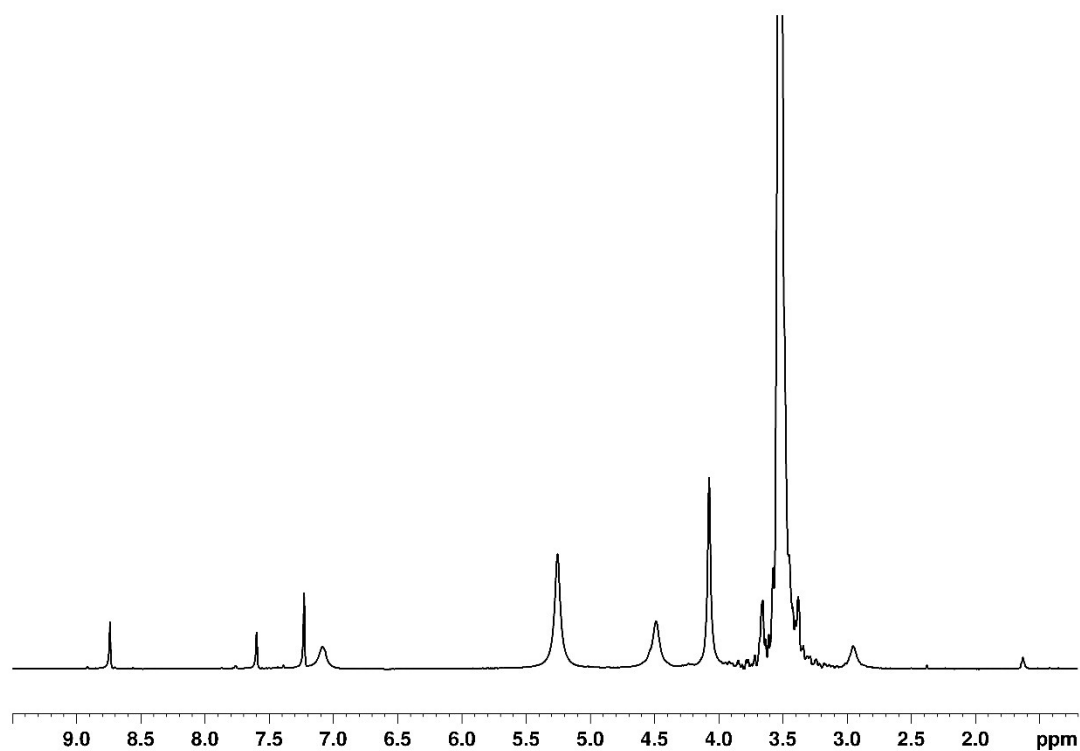
Figure S12: ^{1}H{^{31}P} NMR spectrum of a d_5-pyridine solution of [K(18-crown-6)][**3**].
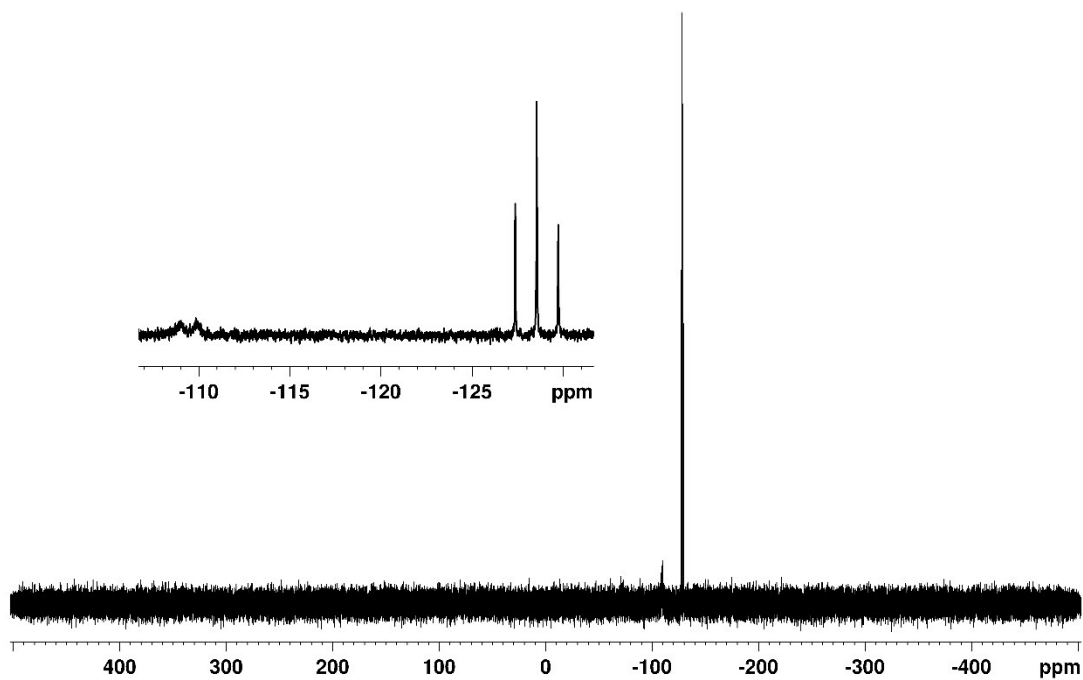
Figure S13: ^{31}P NMR spectrum of a d_5-pyridine solution of [K(18-crown-6)][**3**].
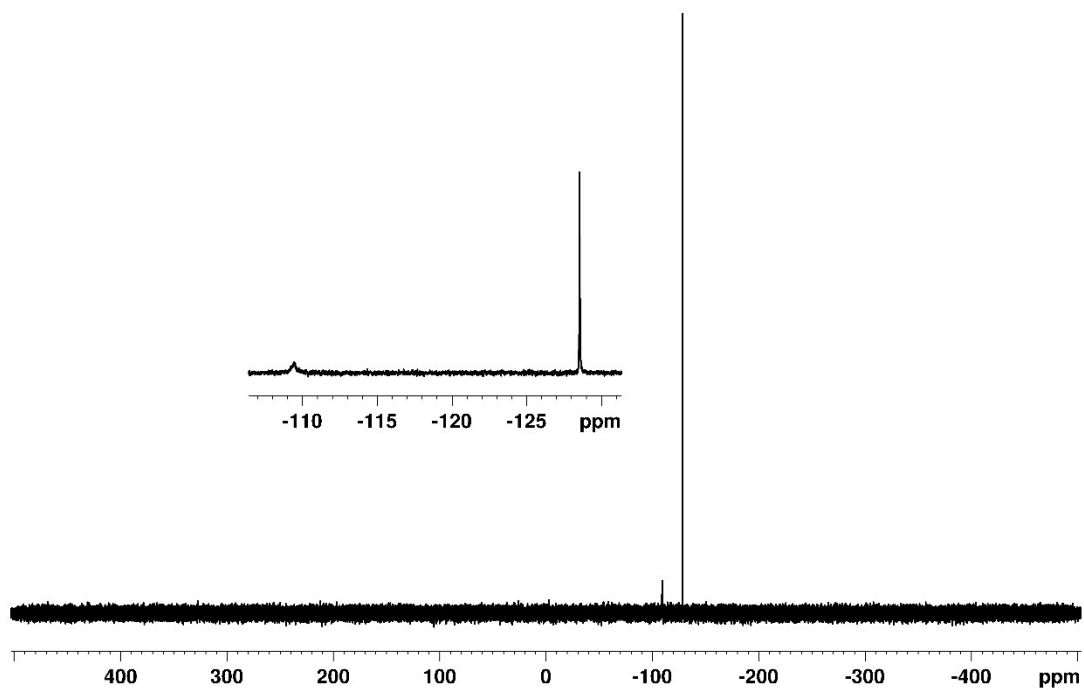
Figure S14: $^{31}P\{^{1}H\}$ NMR spectrum of a d_5-pyridine solution of [K(18-crown-6)][**3**].
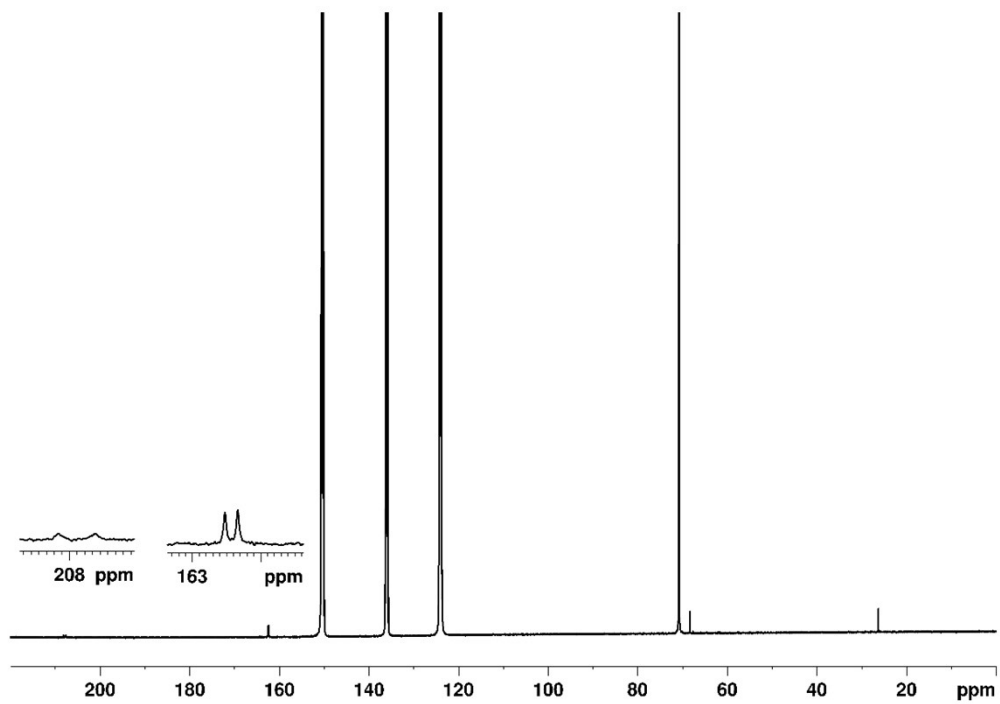
Figure S15: $^{13}C\{^{1}H\}$ NMR spectrum of a d_5-pyridine solution of [K(18-crown-6)][**3**].
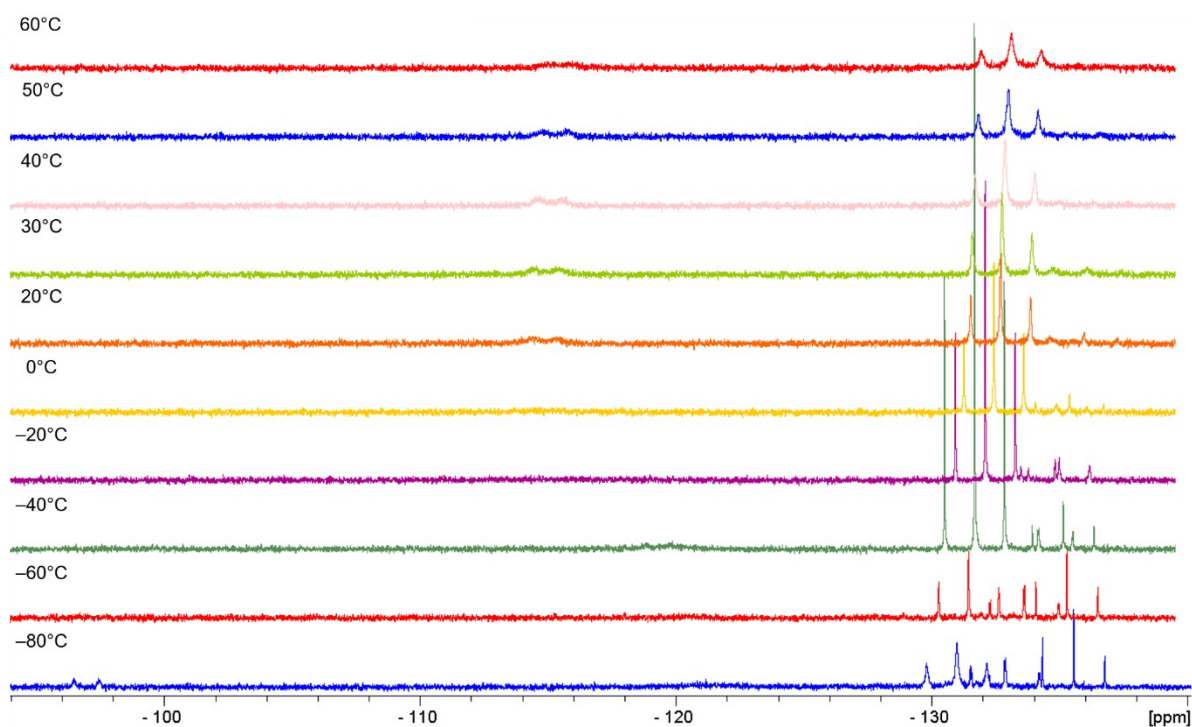
Figure S16: Plots of the variable temperature ^{31}P NMR experiment for the reaction of **1**, KHMDS and 18-crown-6 in d_8-THF from −80 °C to +60 °C taking 20 °C increments up to 20 °C and 10 °C increments between 20 °C and 60 °C.
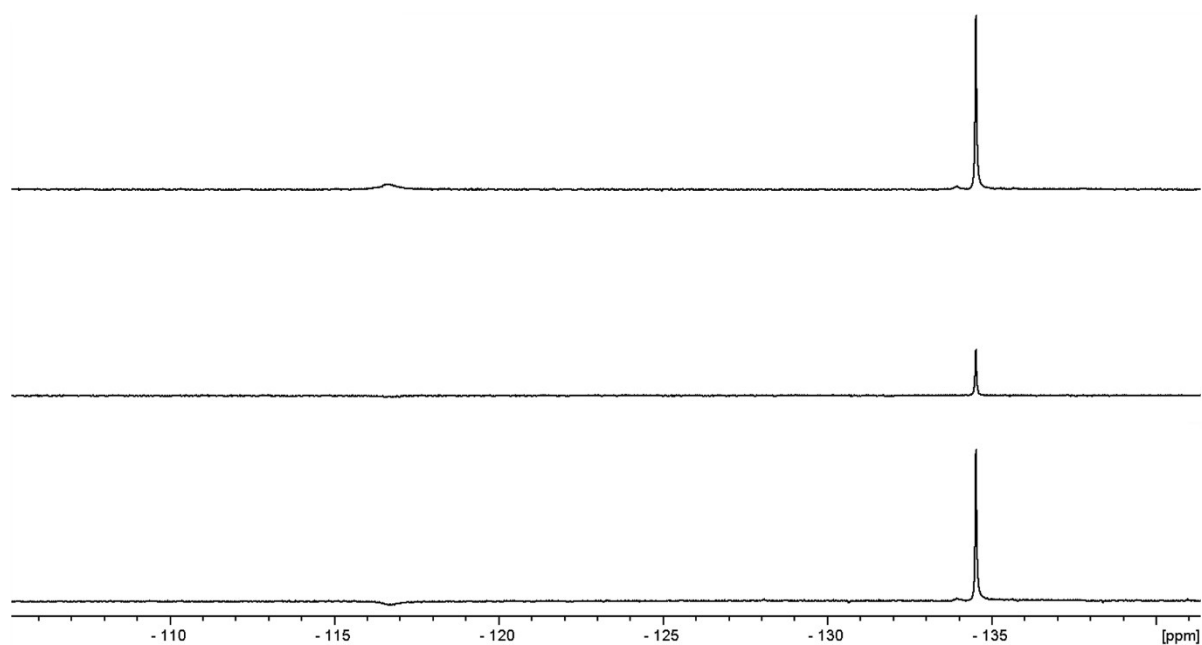
Figure S17: ^{31}P{^{1}H} selective inversion 1D-EXSY spectra of a d_8-THF solution of [K(18-crown-6)][**3**] at room temperature with initial inversion of the phosphide signal (bottom) followed by relaxation over time until the equilibrium (top).

[K(18-crown-6)]$_2$[**4**]

Compound **2** (7 mg, 0.0389 mmol), KHMDS (15.5 mg, 0.0777 mmol) and 18-crown-6 (20.6 mg, 0.0777 mmol) were weighed into an air-tight NMR tube. d_5-pyridine (0.4 mL) was added to the solids and the resulting bright yellow solution as analysed by multi-elemental NMR spectroscopy.

¹H NMR (499.9 MHz, d_5-pyridine): δ (ppm) 6.46 (br s , 2H; N*H*), 3.79 (m; residual THF), 3.77 (m; C*H*$_2$), 3.55 (s; 18-crown-6), 2.78 (d, 2H, $^1J_{H-P}$ = 150 Hz; P*H*), 1.48 (bs; residual THF), 0.16 (s; HMDS).

¹H{³¹P} NMR (499.9 MHz, d_5-pyridine): δ (ppm) 2.78 (s; P*H*); other resonances unchanged from ¹H NMR spectrum.

³¹P NMR (162.0 MHz, d_5-pyridine): δ (ppm) −98.8 (br d, $^1J_{P-H}$ = 150 Hz; P*H*), −256.5 (br t, $^1J_{P-H}$ = 134 Hz; KP*H*$_2$ impurity).

³¹P{¹H} NMR (162.0 MHz, d_5-pyridine): δ (ppm) −98.8 (br s), −256.5 (br s).

¹³C{¹H} NMR (100.6 MHz, d_5-pyridine): δ (ppm) 203.79 ($^1J_{C-P}$ = 59 Hz; P*C*(O)), 70.79 (s; 18-crown-6), 43.28 (s, *C*H$_2$), 3.22 (s; HMDS).
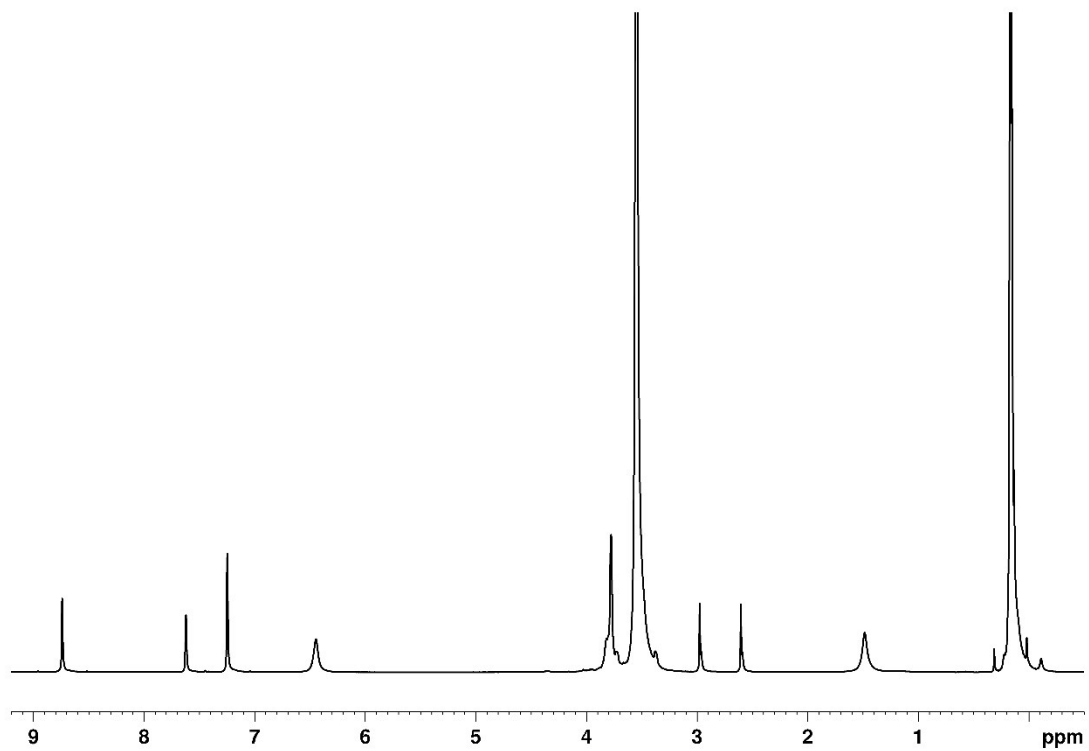
Figure S18: ^{1}H NMR spectrum of a d_5-pyridine solution of [K(18-crown-6)]$_2$[**4**].
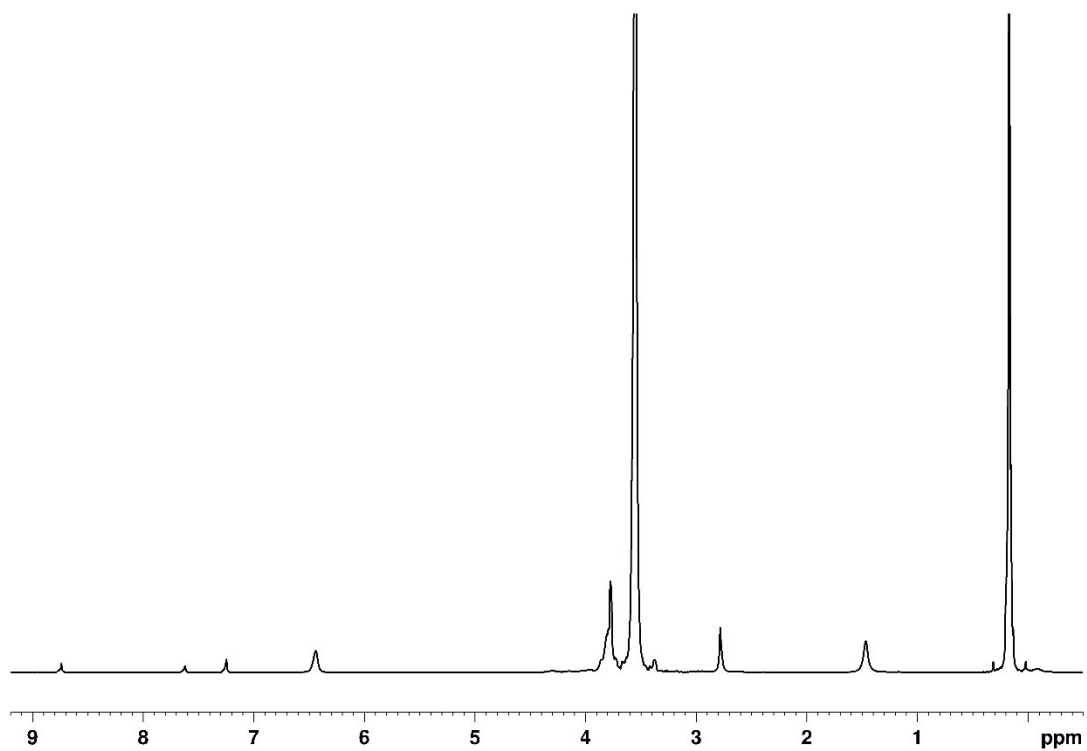
Figure S19: ^{1}H{^{31}P} NMR spectrum of a d_5-pyridine solution of [K(18-crown-6)]$_2$[**4**].
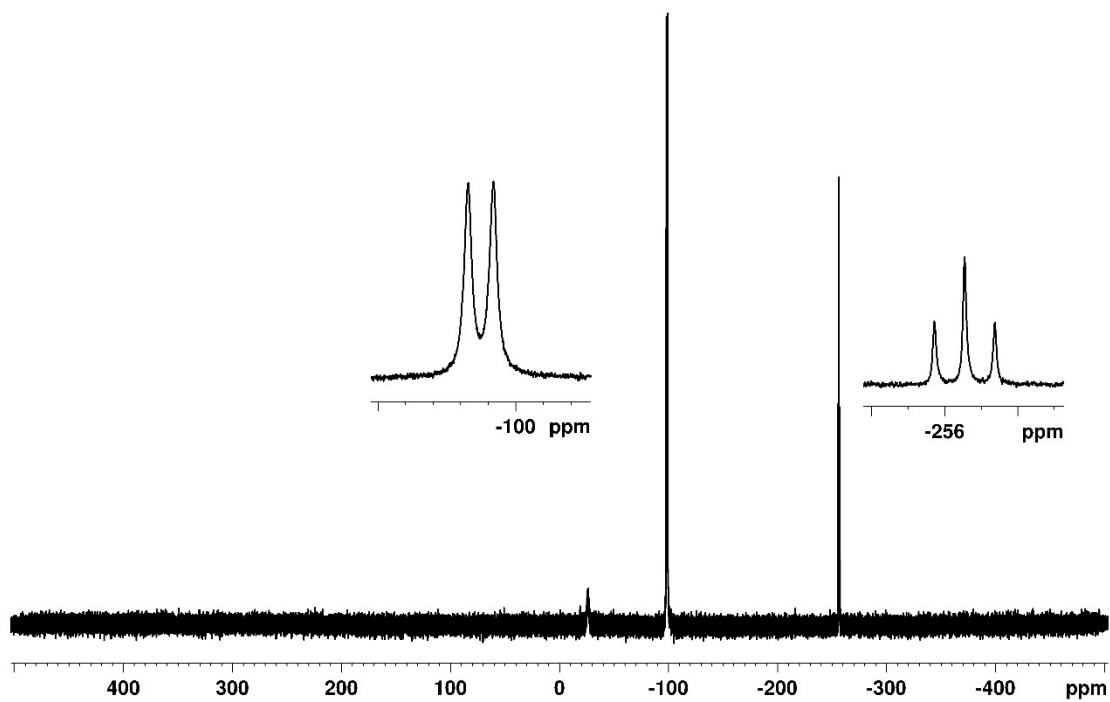
Figure S20: ^{31}P NMR spectrum of a d_5-pyridine solution of [K(18-crown-6)]$_2$[**4**].
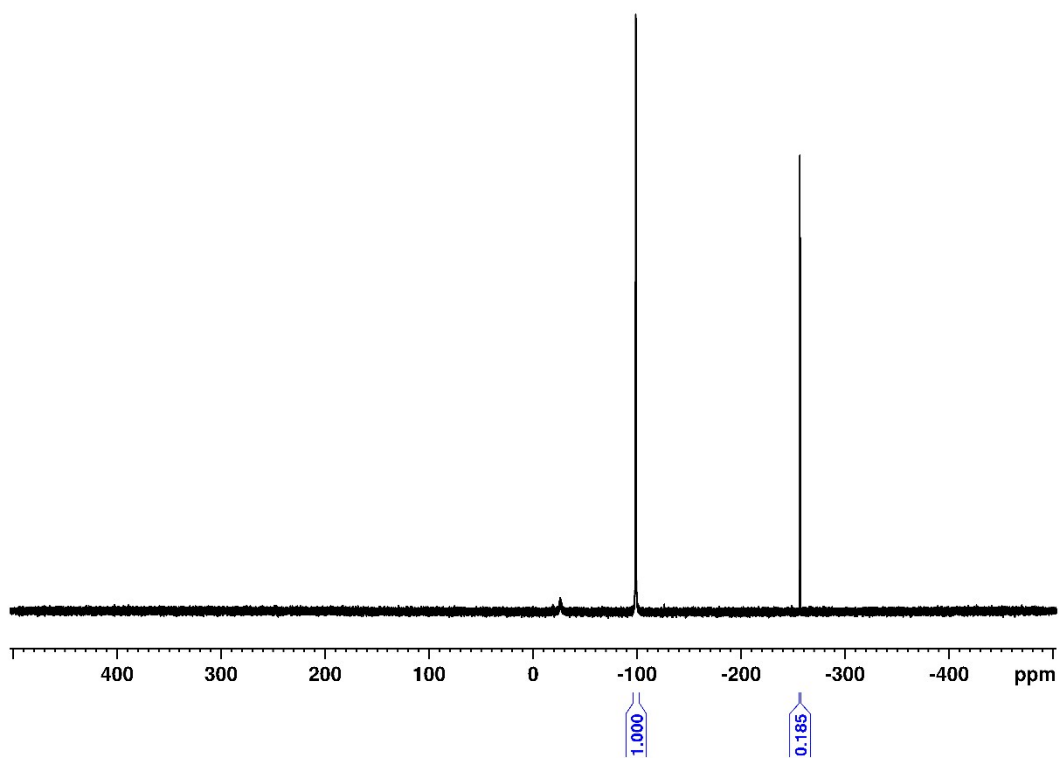
Figure S21: ^{31}P{^{1}H} NMR spectrum of a d_5-pyridine solution of [K(18-crown-6)]$_2$[**4**].
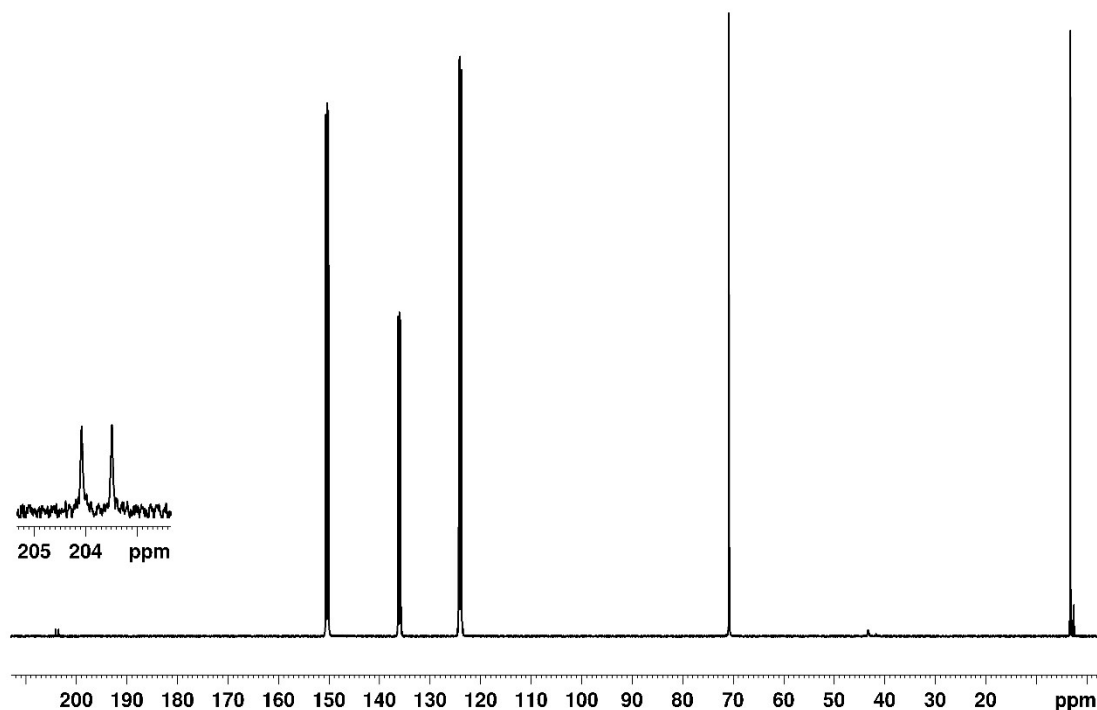
Figure S22: $^{13}C\{^1H\}$ NMR spectrum of a d_5-pyridine solution of [K(18-crown-6)]$_2$[**4**].

<u>Methylated hydrazine mono-phosphinecarboxamide (**5**)</u>

MeI (13.2 μL, 0.2127 mmol) was added to a THF (4 mL) solution of [K(18-crown-6)][**3**] (83.3 mg, 0.2127 mmol) and allowed to stir for 40 minutes. Volatiles were removed under vacuum at 0°C. Toluene (4 mL) was added and the mixture was kept in the freezer for two days. The colourless solution was filtered, and the toluene removed under vacuum at 0 °C to yield the product as a white solid (52.8 mg, 67% yield).

^{1}H NMR (499.9 MHz, d_5-pyridine): δ (ppm) 10.61 (br s, NH, **5a**), 9.74 (br s, NH, **5b**), 5.29 (br s, NH_2, **5a**, **5b**), 4.60 (dq, $^1J_{P-H}$ = 228 Hz, $^3J_{H-H}$ = 7 Hz, PHCH$_3$, **5b**), 4.04 (dq, $^1J_{P-H}$ = 207 Hz, $^3J_{H-H}$ = 8 Hz, PHCH$_3$, **5a**), 3.65 (s, 18-crown-6), 2.24 (s, residual toluene), 1.37 (dd, $^2J_{H-P}$ = 3 Hz, $^3J_{H-H}$ = 7 Hz, PHCH_3, **5a**), 1.36 (dd, $^2J_{H-P}$ = 4 Hz, $^3J_{H-H}$ = 7 Hz, PHCH_3, **5b**).

¹H{³¹P} NMR (499.9 MHz, d_5-pyridine): δ (ppm) 4.60 (q, $^3J_{H-H}$ = 7 Hz; P*H*CH₃, **5b**), 4.04 (q, $^3J_{H-H}$ = 8 Hz; P*H*CH₃, **5a**), 1.37 (d, $^3J_{H-H}$ = 7 Hz, PHC*H₃*, **5a**), 1.36 (d, $^3J_{H-H}$ = 7 Hz, PHC*H₃*, **5b**), other resonances unchanged from ¹H NMR spectrum.

³¹P NMR (162.0 MHz, d_5-pyridine): δ (ppm) –85.4 (dq, $^1J_{P-H}$ = 207 Hz; $^2J_{P-H}$ = 3 Hz; *P*HCH₃, **5a**), –86.8 (dm, $^1J_{P-H}$ = 228 Hz, $^2J_{P-H}$ = 3 Hz; *P*HCH₃, **5b**), –44.2 (bs; *P*(CH₃)₂).

³¹P{¹H} NMR (162.0 MHz, d_5-pyridine): δ (ppm) –85.4 (s; *P*HCH₃, **5a**), –86.8 (s; *P*HCH₃, **5b**), –44.2 (s; *P*(CH₃)₂).

¹³C{¹H} NMR (125.8 MHz, d_5-pyridine): δ (ppm) 185.08 (d, $^1J_{C-P}$ = 6 Hz; P*C*(O), **5b**), 177.68 (d, $^1J_{C-P}$ = 13 Hz; P*C*(O), **5a**,), 71.35 (s; 18-crown-6), 11.49 (d, $^1J_{C-P}$ = 12 Hz; P(*C*H₃)₂), 1.83 (d, $^1J_{C-P}$ = 6 Hz; **5b**), 1.53 (d, $^1J_{C-P}$ = 9 Hz; PH*C*H₃, **5a**) .

Figure S23: ¹H NMR spectrum of a d_5-pyridine solution of **5**.

Figure S24: ^{1}H{^{31}P} NMR spectrum of a d_5-pyridine solution of **5**.

Figure S25: ^{31}P NMR spectrum of a d_5-pyridine solution of **5**.

Figure S26: $^{31}P\{^1H\}$ NMR spectrum of a d_5-pyridine solution of **5**.

Figure S27: $^{13}C\{^1H\}$ NMR spectrum of a d_5-pyridine solution of **5**.

Figure S28: ^{1}H-^{31}P HMBC NMR spectrum of a d_5-pyridine solution of **5**.

Methylated ethylenediamine *bis*-phosphinecarboxamide (**6**)

Compound **2** (40.0 mg, 0.222 mmol) was dissolved in 3 mL of THF in a Schlenk tube. MeI (27.6 μL, 0.444) was added and the mixture was allowed to stir for 10 minutes. KHMDS (88.6 mg, 0.444 mmol) was weighed into another Schlenk and dissolved it in 4 mL of THF. The KHMDS solution was added to the **2**/MeI mixture. A white solid precipitated as the addition was taking place. The mixture was stirred for 3 hours. The colourless solution was filtered and kept in the freezer. The resulting crystalline solid was filtered and dried under vacuum to yield a mixture of the three compounds as a white solid (38.4 mg).

^{1}H NMR (499.9 MHz, d_5-pyridine): δ (ppm) 9.53 (br s; NHC(O)PH$_2$, **2**), 9.34 (br s; NHC(O)PH(CH$_3$), **6a**), 8.97 (bs; PH$_2$C(O)NH(CH$_2$)$_2$NHC(O)P(CH$_3$)$_2$), 4.022 and 4.016 (dq, $^1J_{H–P}$ = 207 Hz, $^3J_{H–H}$ = 7 Hz; PHCH$_3$, **6a**), 3.74 (m, (CH_2)$_2$, **6a**), 3.73 (d; $^1J_{P–H}$ = 207 Hz, PH_2, PH$_2$C(O)NH(CH$_2$)$_2$NHC(O)P(CH$_3$)$_2$), 3.72 (m, (CH_2)$_2$, PH$_2$C(O)NH(CH_2)$_2$NHC(O)P(CH$_3$)$_2$),

3.69 (m; (CH_2)$_2$, **2**), 1.35 (d, $^2J_{H–P}$ = 3 Hz, P(CH_3)$_2$, PH$_2$C(O)NH(CH_2)$_2$NHC(O)P(CH_3)$_2$), 1.34 (dd, $^2J_{H–P}$ = 3 Hz, $^3J_{H–H}$ = 7 Hz; NHC(O)PH(CH_3) **6a**).

^{1}H{^{31}P} NMR (499.9 MHz, d_5-pyridine): δ (ppm) 4.022 and 4.016 (q, $^3J_{H–H}$ = 7 Hz; PHCH$_3$, **6a**), 3.73 (s; PH_2, PH_2C(O)NH(CH$_2$)$_2$NHC(O)P(CH$_3$)$_2$), 1.35 (s; P(CH_3)$_2$, PH$_2$C(O)NH(CH_2)$_2$NHC(O)P(CH_3)$_2$), 1.34 (d; $^2J_{H–H}$ = 7 Hz, NHC(O)PH(CH_3) **6a**), other resonances unchanged from ^{1}H NMR spectrum.

^{31}P NMR (162.0 MHz, d_5-pyridine): δ (ppm) –41.06 and –41.09 (sep; P(CH$_3$)$_2$, PH$_2$C(O)NH(CH$_2$)$_2$NHC(O)P(CH$_3$)$_2$), –81.06 (dq, $^1J_{P–H}$ = 207 Hz, $^3J_{H–H}$ = 3 Hz; PHCH$_3$, **6b**), –81.08 and –81.11 (dq, $^1J_{P–H}$ = 207 Hz, $^3J_{H–H}$ = 3 Hz; PHCH$_3$, **6a**), –132.7 (t, $^1J_{P–H}$ = 207 Hz; PH$_2$, PH$_2$C(O)NH(CH$_2$)$_2$NHC(O)P(CH$_3$)$_2$).

^{31}P{^{1}H} NMR (162.0 MHz, d_5-pyridine): δ (ppm) –41.06 and –41.09 (s; P(CH$_3$)$_2$, PH$_2$C(O)NH(CH$_2$)$_2$NHC(O)P(CH$_3$)$_2$), –81.06 (s; PHCH$_3$, **6b**), –81.08 and –81.11 (s; PHCH$_3$, **6a**), –132.7 (s, PH$_2$, PH$_2$C(O)NH(CH$_2$)$_2$NHC(O)P(CH$_3$)$_2$).

^{13}C{^{1}H} NMR (125.8 MHz, d_5-pyridine): δ (ppm) 183.11 and 182.94 (d, $^1J_{C–P}$ = 16 Hz; (CH$_3$)$_2$PC(O), PH$_2$$C$(O)NH(CH$_2$)$_2NHC$(O)P(CH$_3$)$_2$), 178.95 (d, $^1J_{C–P}$ = 11 Hz; PC(O), **6b**); 178.82 and 178.80 (d, $^1J_{C–P}$ = 11 Hz; (CH$_3$)HPC(O), **6a**), 173.58 (d, $^1J_{C–P}$ = 7 Hz; H$_2$PC(O), **2**), 40.82 (s; CH$_2$, **6a**), 40.76 (s; CH$_2$, **2**), 11.63 (d, $^1J_{C–P}$ = 12 Hz; P(CH$_3$)$_2$, PH$_2$C(O)NH(CH$_2$)$_2$NHC(O)P(CH$_3$)$_2$), 1.74 (d, $^1J_{C–P}$ = 8 Hz, PHCH$_3$, **6a**).
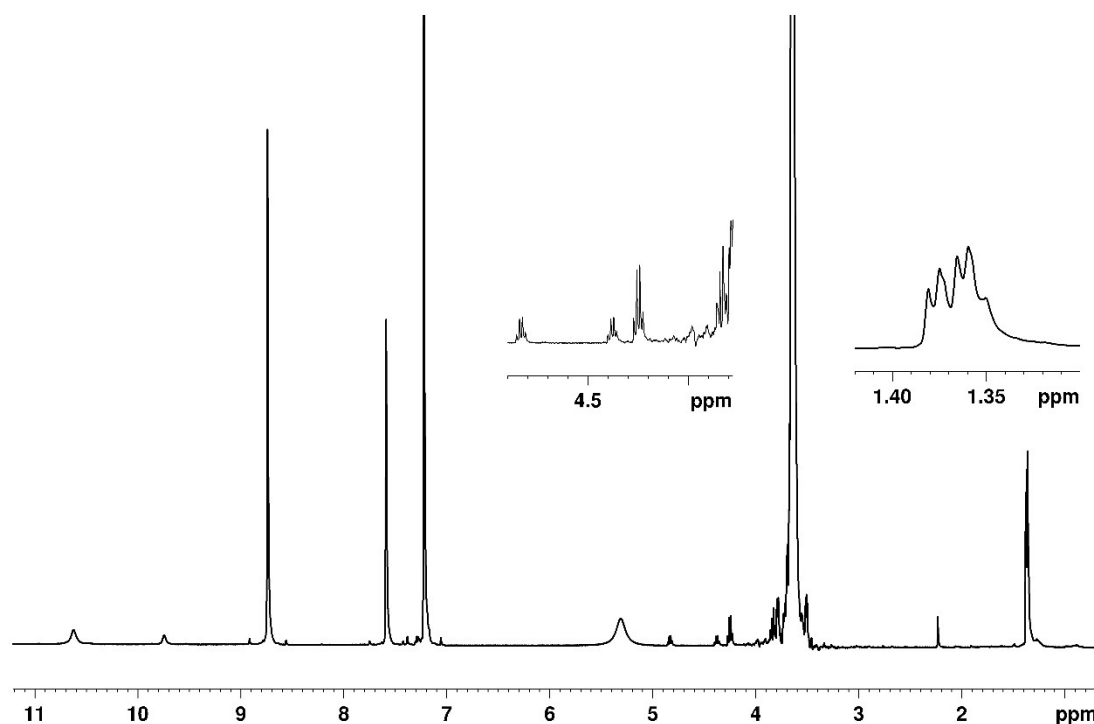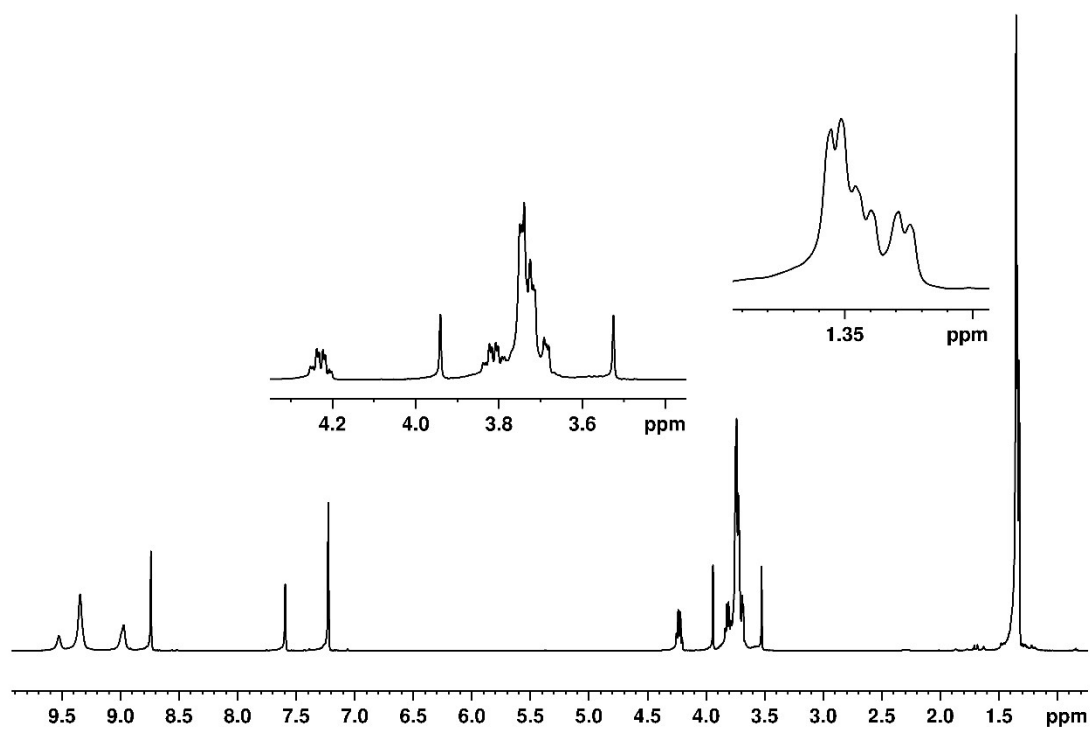
Figure S29: ^{1}H NMR spectrum of a d_5-pyridine solution of **6**.
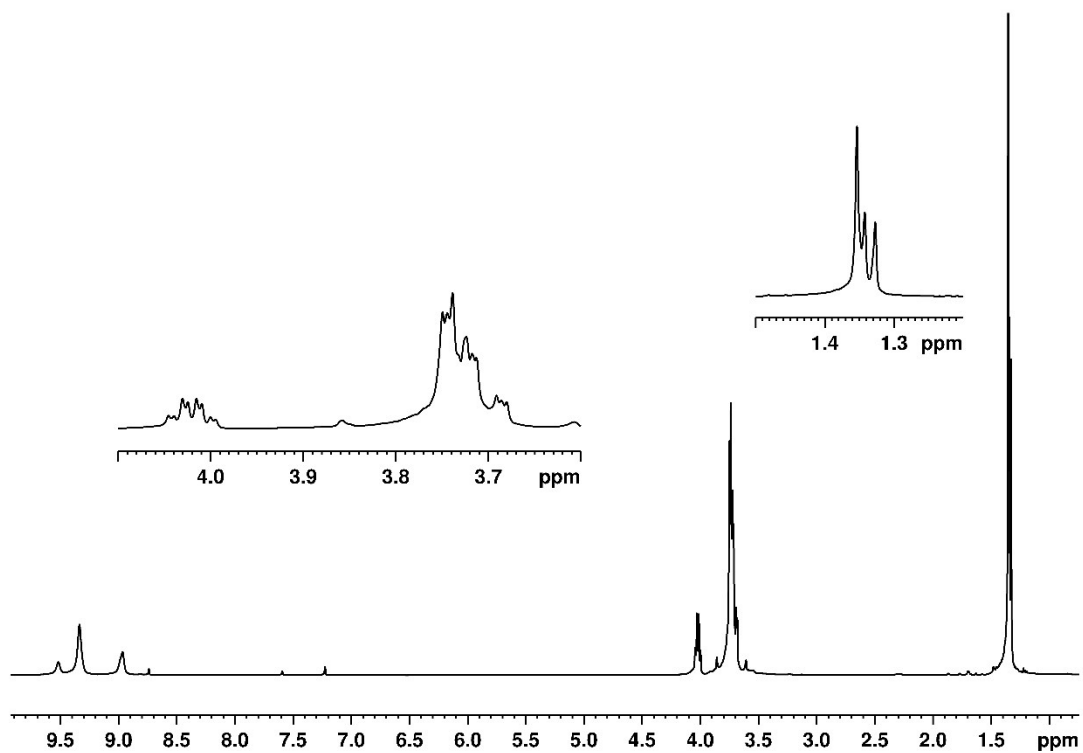
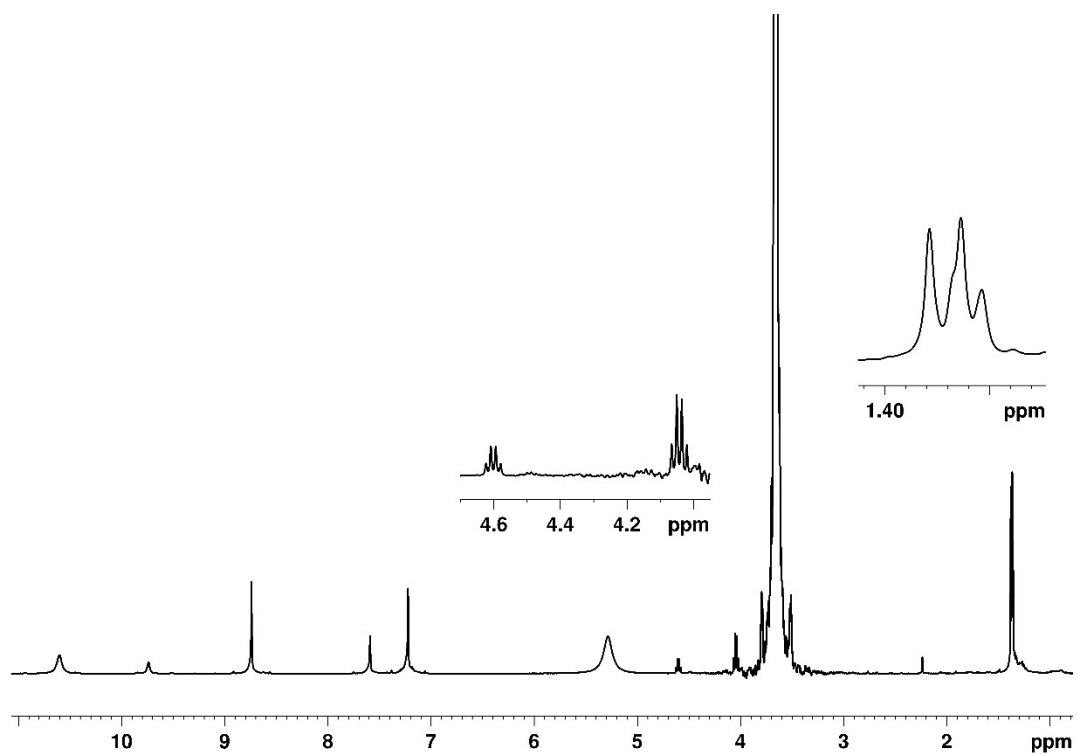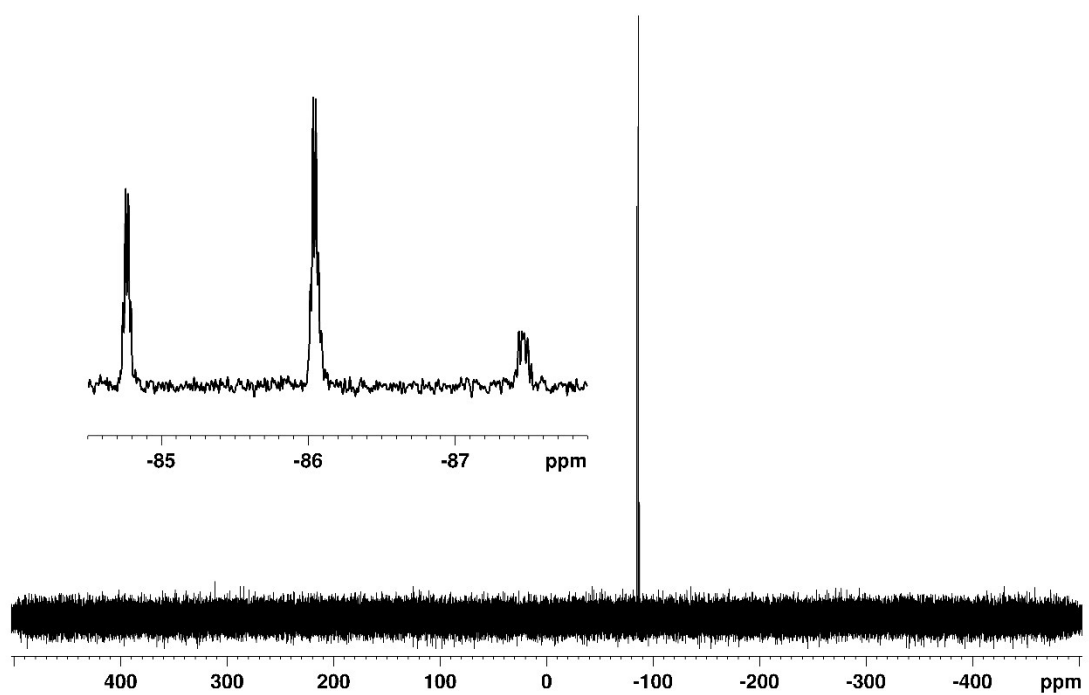**Figure S30:** ^{1}H{^{31}P} NMR spectrum of a d_5-pyridine solution of **6**.
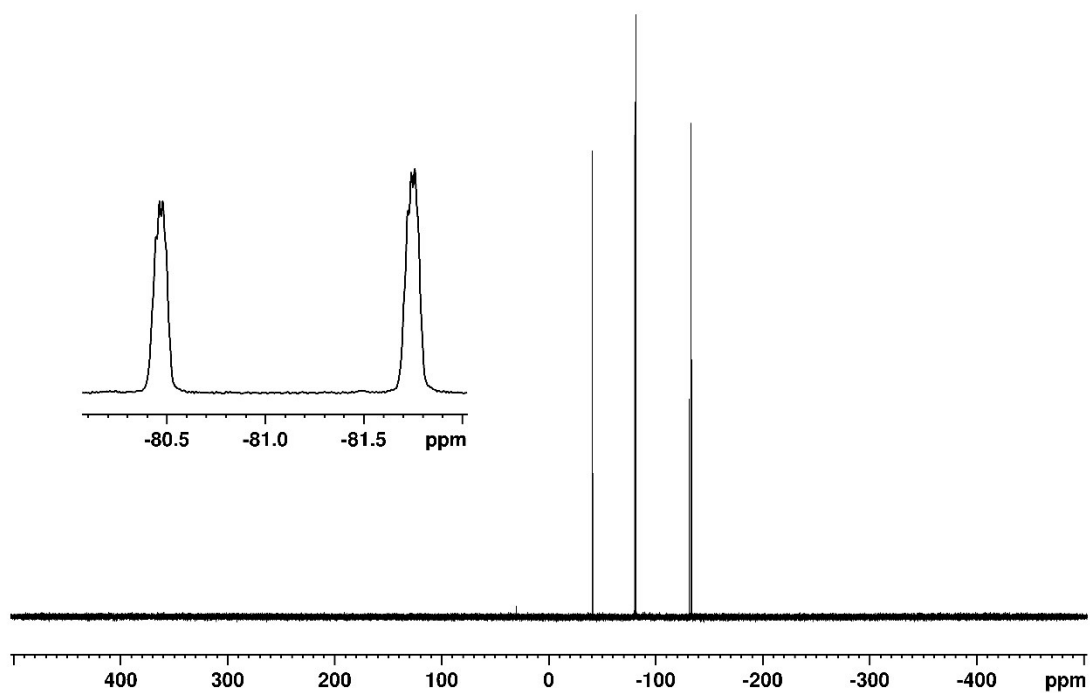
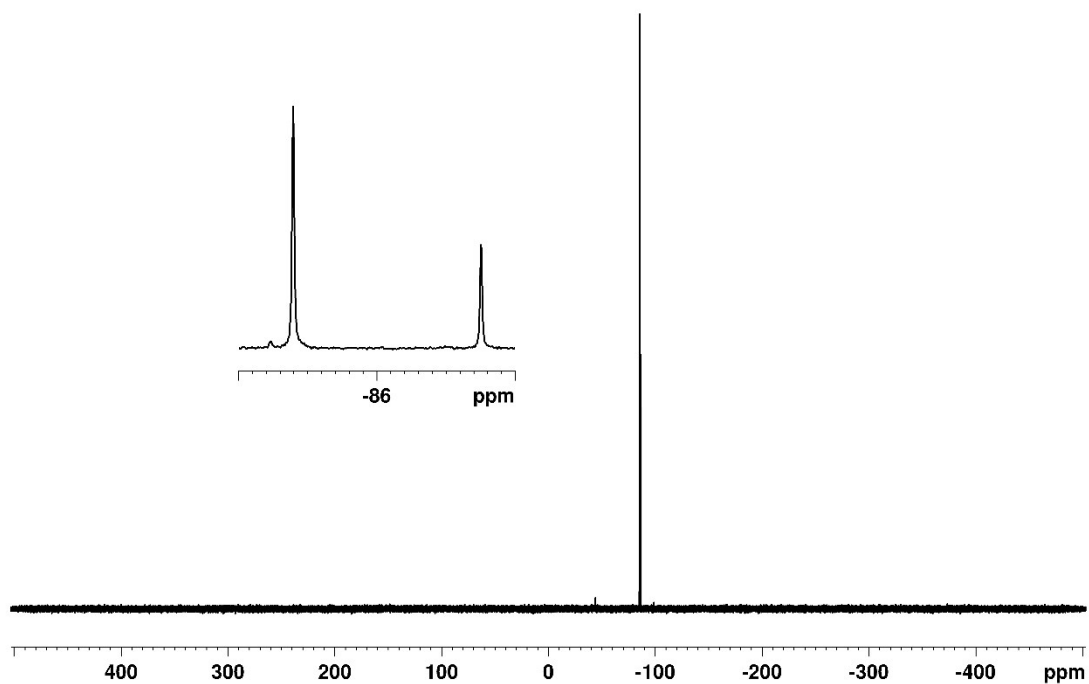**Figure S31:** ^{31}P NMR spectrum of a d_5-pyridine solution of **6**.
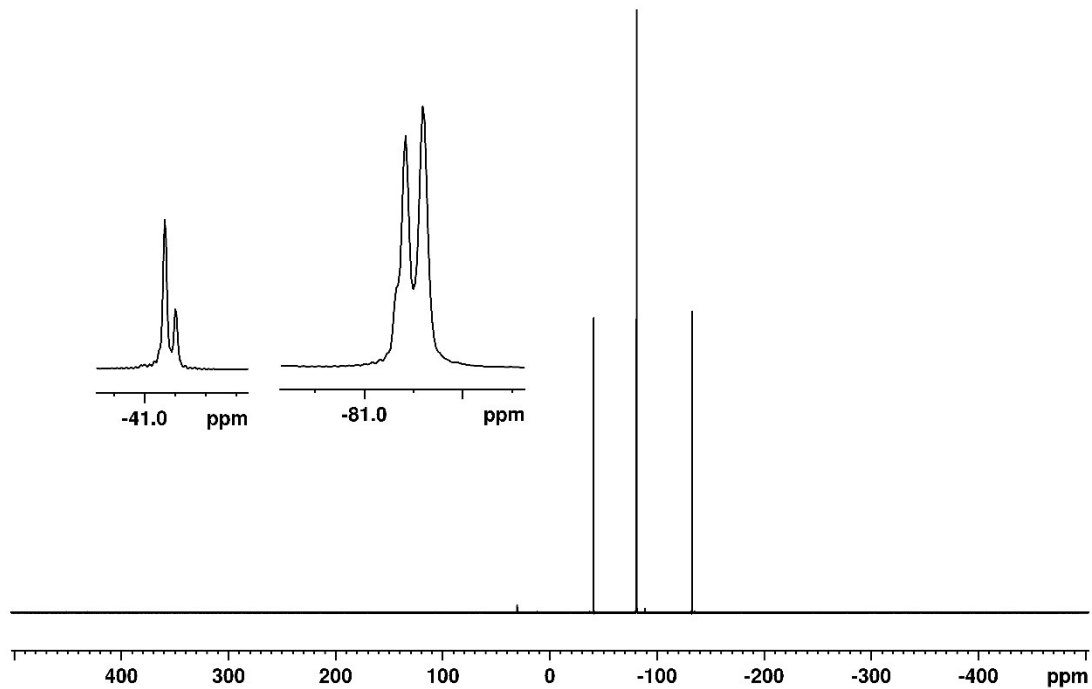
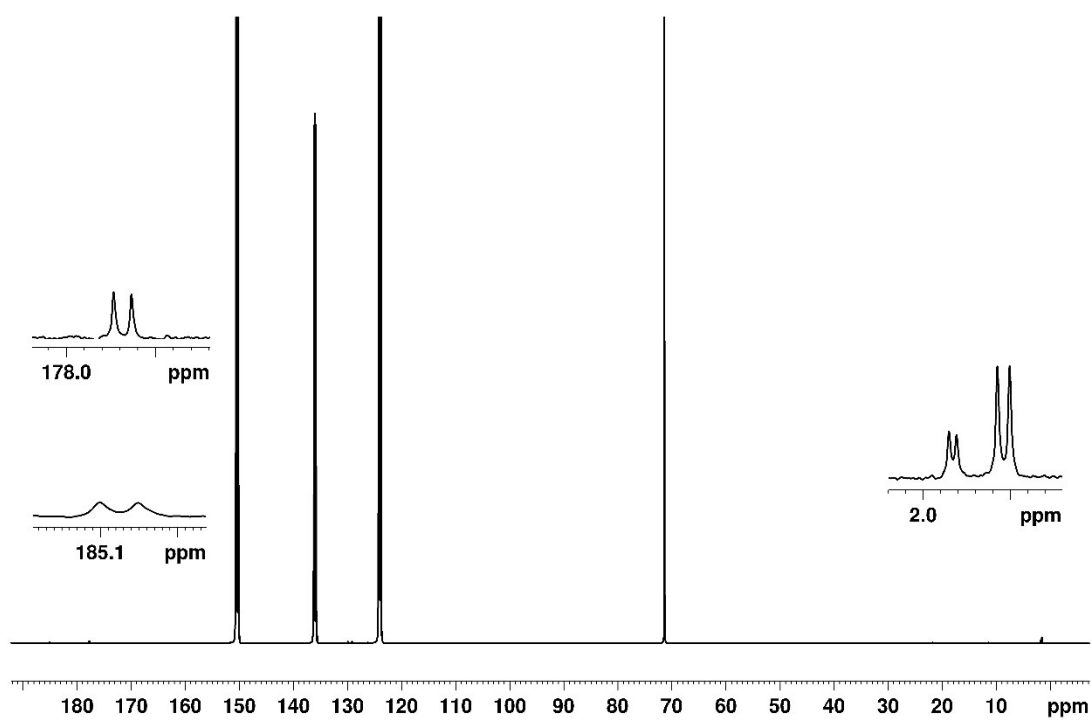**Figure S32:** ^{31}P{^{1}H} NMR spectrum of a d_5-pyridine solution of **6**.
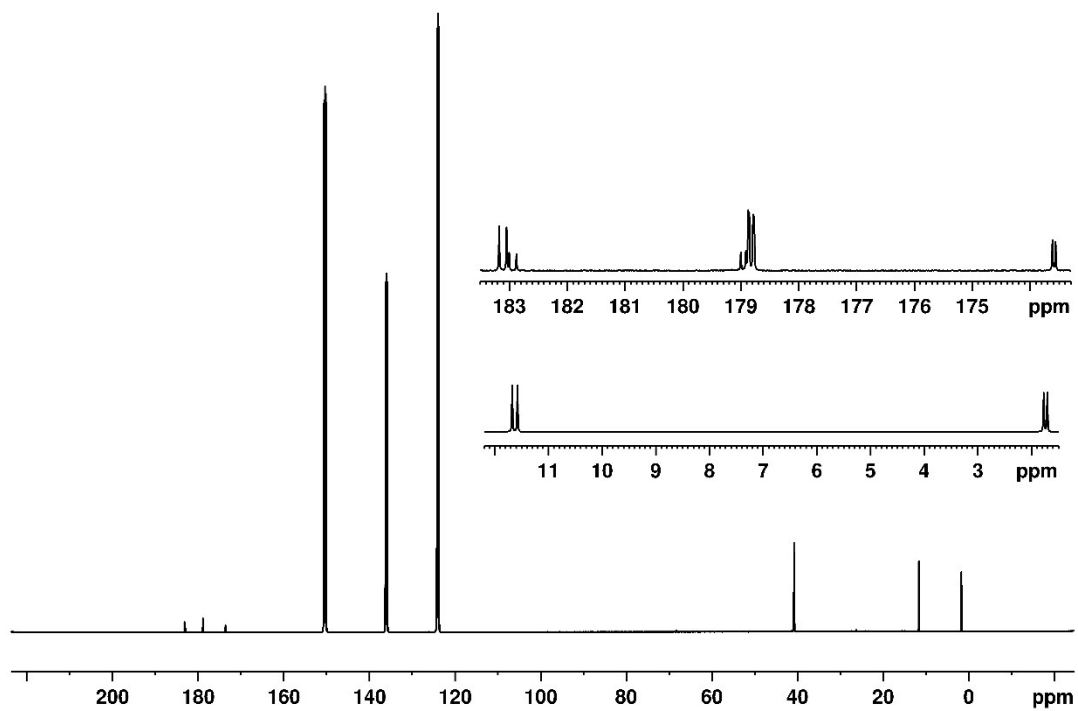
Figure S33: $^{13}C\{^1H\}$ NMR spectrum of a d_5-pyridine solution of **6**.

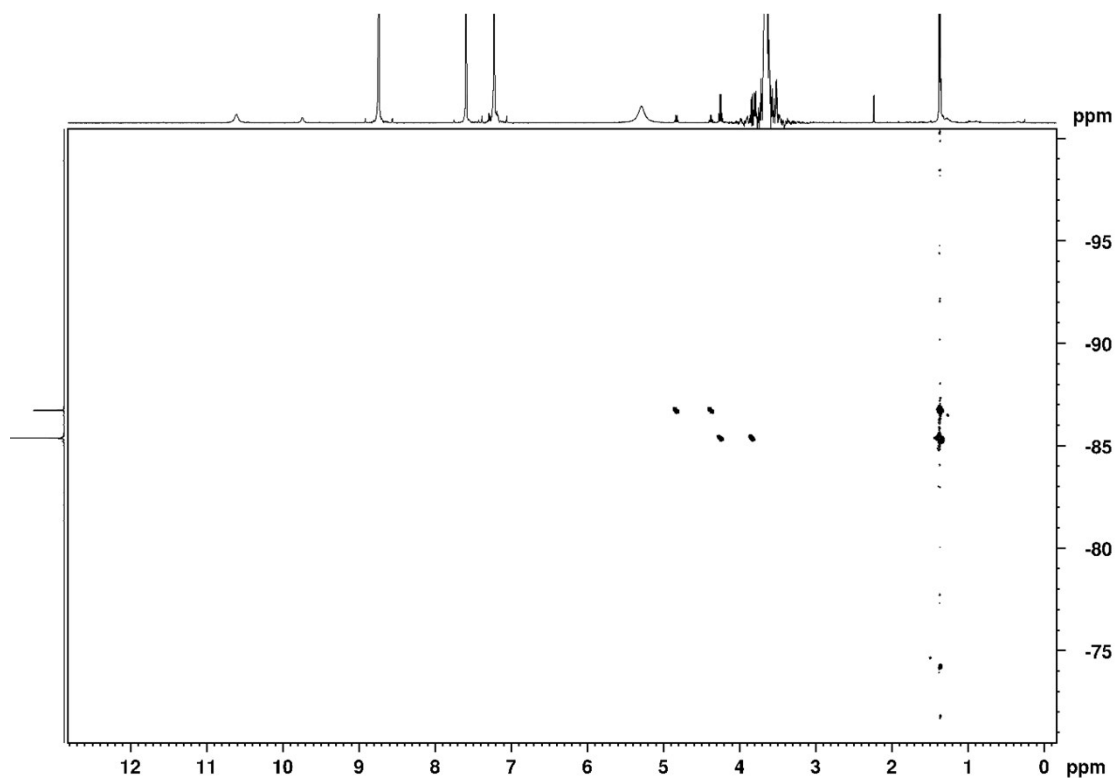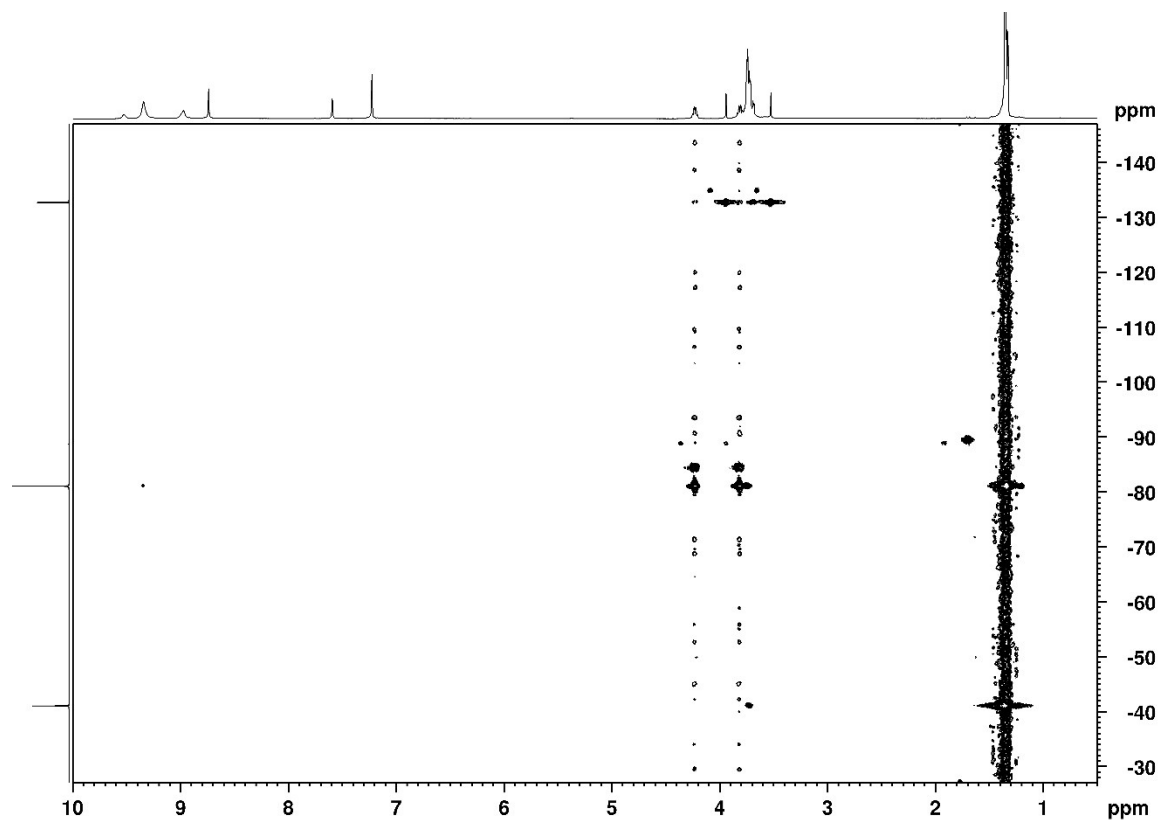**Figure S34:** $^1H-^{31}P$ HMBC NMR spectrum of a d_5-pyridine solution of **6**.

2. Single crystal X-ray diffraction data

Single-crystal X-ray diffraction data were collected using an Oxford Diffraction Supernova dual-source diffractometer equipped with a 135 mm Atlas CCD area detector. Crystals were selected under Paratone-N oil, mounted on micromount loops, and quench-cooled using an Oxford Cryosystems open flow N_2 cooling device. Data were collected at 150 K using mirror monochromated Cu Kα radiation (λ = 1.5418 Å; Oxford Diffraction Supernova) or graphite-monochromated Mo Kα radiation (λ = 0.71073 Å; Enraf-Nonius kappa-CCD). Data collected on the Oxford Diffraction Supernova diffractometer were processed using the CrysAlisPro package, including unit cell parameter refinement and interframe scaling (which was carried out using SCALE3 ABSPACK within CrysAlisPro). Equivalent reflections were merged, and direct methods or using the charge flipping algorithm as implemented in the program SUPERFLIP and refined on F^2 using the SHELXL 97-2 package.

Table S2: Selected X-ray data collection and refinement parameters for **1a**, **1b**·(18-crown-6)$_{0.5}$, **2** and [K(18-crown-6)][*cis-cis*-**3a**].

	1a	**1b**·(18-crown-6)$_{0.5}$	**2**	[K(18-crown-6)][*cis-cis*-**3a**]
Formula	CH$_5$N$_2$OP	C$_7$H$_{17}$N$_2$O$_4$P	C$_4$H$_{10}$N$_2$O$_2$P$_2$	C$_{13}$H$_{28}$KN$_2$O7P
CCDC	2076831	2076832	2076833	2076834
Fw [g mol^{-1}]	92.04	224.19	180.08	394.44
Crystal system	monoclinic	monoclinic	monoclinic	orthorhombic
Space group	$P2_1/c$	$P2_1/c$	$P2_1/n$	$Pna2_1$
a (Å)	25.025(2)	13.9885(2)	7.1091(2)	16.5692(3)
b (Å)	4.8946(4)	11.78140(10)	4.91330(10)	8.8974(2)
c (Å)	6.9706(10)	14.7581(2)	12.5171(3)	12.9189(3)
α (°)	90	90	90	90
β (°)	93.901(10)	109.5020(10)	92.067(2)	90
γ (°)	90	90	90	90
V (Å^3)	851.85(16)	2292.66(5)	436.927(18)	1904.54(7)
Z	8	8	2	4
Radiation, λ (Å)	Cu Kα, 1.54184	Cu Kα, 1.54184	Cu Kα, 1.54184	Mo Kα, 0.71073
Temp (K)	150(2)	150(2)	150(2)	150(2)
ρ_{calc} (g cm^{-3})	1.435	1.299	1.369	1.376
μ (mm^{-1})	4.342	2.122	4.156	0.398
Reflections collected	5153	22090	3760	25455
Independent reflections	1500	4757	896	4693
Parameters	130	293	66	233
R(int)	0.0636	0.0152	0.0148	0.0351
R1/wR2,[a] I ≥ 2σI (%)	7.88/21.02	5.51/13.17	2.38/6.17	2.92/5.87
R1/wR2,[a] all data (%)	10.63/22.03	5.66/13.29	2.47/6.20	3.49/6.20
GOF	1.127	1.038	1.134	1.059

R1 = [Σ||F$_o$| − |F$_c$||]/Σ|F$_o$|; wR2 = {[Σw[(F$_o$)^2 − (F$_c$)^2]^2]/[Σw(F$_o$^{2})^2}$^{1/2}$; w = [σ^2(F$_o$)^2 + (AP)^2 + BP]$^{-1}$, where P = [(F$_o$)^2 + 2(F$_c$)^2]/3 and the A and B values are 0.0798 and 4.95 for **1a**, 0.0535 and 3.57 for **1b**·(18-crown-6)$_{0.5}$, 0.0327 and 0.11 for **2**, and 0.0232 and 0.42 for [K(18-crown-6)][*cis-cis*-**3a**].

Table S3: Bond distances (Å) for the two distinct molecules of **1a** in the asymmetric unit.

Bond distances (Å)	**1a_1**	**1a_2**
P1–C1	1.859(6)	1.868(7)
C1–O1	1.220(8)	1.228(8)
C1–N1	1.339(8)	1.326(8)
N1–N2	1.432(7)	1.429(8)

Table S4: Bond angles (°) for the two distinct molecules of **1a** in the asymmetric unit.

Bond angles (°)	**1a_1**	**1a_2**
O1–C1–N1	123.7(6)	124.6(6)
O1–C1–P1	120.0(5)	118.4(5)
N1–C1–P1	116.1(5)	116.8(5)
C1–N1–N2	121.4(5)	121.3(5)

Table S5: Bond distances (Å) for the two distinct molecules of **1b** in the asymmetric unit.

Bond distances (Å)	**1b_1**	**1b_2**
P1–C1	1.875(2)	1.863(2)
C1–O1	1.223(3)	1.220(3)
C1–N1	1.341(3)	1.337(3)
N1–N2	1.405(3)	1.408(3)
O101–C102	1.421(3)	1.420(3)
O101–C101	1.424(3)	1.426(3)
O102–C104	1.423(2)	1.422(3)
O102–C103	1.424(3)	1.426(3)
O103–C105	1.425(2)	1.421(3)
O103–C106	1.426(2)	1.423(3)
C101–C106[1]	1.504(3)	1.498(4)

C102–C103	1.499(3)	1.493(3)
C104–C105	1.501(3)	1.493(3)

[1] −x, 1−y, 1−z

Table S6: Selected bond angles (°) for the two distinct molecules of **1b** in the asymmetric unit.

Bond angles (°)	**1b_1**	**1b_2**
O1–C1–N1	123.3(2)	123.4(2)
O1–C1–P1	121.77(17)	122.68(17)
N1–C1–P1	114.73(16)	113.80(16)
C1–N1–N2	118.38(18)	119.00(18)

Table S7: Bond distances (Å) for the half molecule of **2** in the asymmetric unit.

Bond distances (Å)	**2**
P1–C1	1.8633(12)
C1–O1	1.2275(15)
C1–N1	1.3256(15)
N1–C2	1.4549(15)
C2–C2[1]	1.519(2)

[1] −x, 1−y, 1−z

Table S8: Selected bond angles (°) for the half molecule of **2** in the asymmetric unit.

Bond angles (°)	**2**
O1–C1–N1	123.06(11)
O1–C1–P1	118.38(9)
N1–C1–P1	118.47(8)
C1–N1–C2	121.99(10)
N1–C2–C2[1]	111.42(13)

[1] −x, 1−y, 1−z

Table S9: Selected bond distances (Å) for the molecule of [K(18-crown-6)][*cis-cis*-**3a**] in the asymmetric unit.

Bond distances (Å)	*cis*-**3a**
P1–C1	1.792(2)
P1–K1	3.8244(9)
C1–O1	1.248(3)
C1–N1	1.383(3)
C1–K1	3.420(2)
O1–K1	2.679(2)
N1–N2	1.393(3)
N2–K1[1]	2.948(3)

[1] 3/2−x, −1/2+y, ½+z

Table S10: Selected bond angles (°) for the molecule of [K(18-crown-6)][*cis-cis*-**3a**] in the asymmetric unit.

Bond angles (°)	*cis-cis*-**3a**
O1–C1–N1	116.7(2)
O1–C1–P1	128.0(2)
N1–C1–P1	115.26(18)
C1–N1–N2	122.8(2)
C1–O1–K1	116.30(15)

3. Computational details

All calculations were performed the Gaussian09 software package.[2] Geometries were fully optimised without imposing any symmetry constraints. **1a** and **1b** were optimised with the PBE0 functional using a 6-31g(d,p) basis set.[3,4] The final geometry was characterised as a true minima via harmonic frequency calculations. Transition states were located by scanning dihedral angles starting from optimised geometries. Transition states were verified by harmonic

frequency calculations on a single point, which exhibited a single negative frequency. Solvent effects have not been included in the calculations. All quantum chemical results were visualised using the GaussView 6.0.16 software.
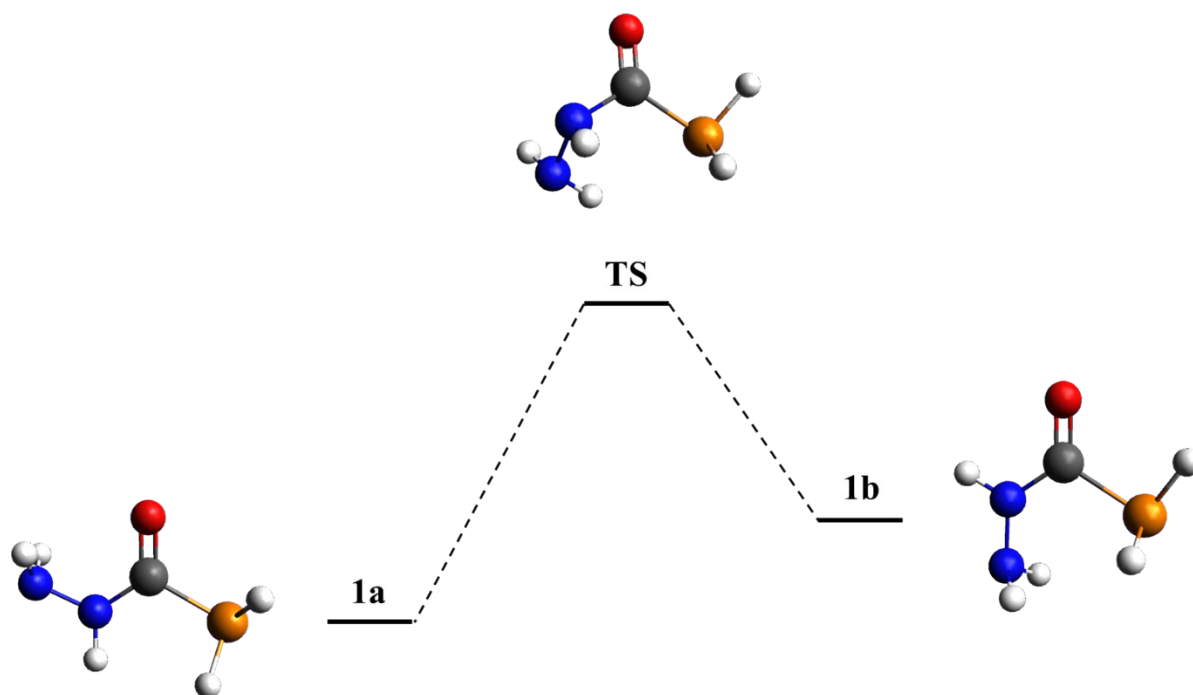
Figure S35: Schematic representation of the potential energy surface for C–N bond rotation. ΔG is given in kJ mol^{-1}: **1a** = 0; **TS** = 92; **1b** = 11.

Coordinates [Å] for the optimized geometry of **1a**.

Atom	x	y	z
N	-2.30069600	-0.41169200	0.01694000
H	-2.52877100	0.09181900	-0.83733200
H	-2.46809700	0.24570800	0.77601200
N	-0.93427800	-0.69081200	-0.00840900
H	-0.68398000	-1.65920900	0.10766900
C	-0.00378100	0.30001800	0.00357400
O	-0.30070700	1.48025100	0.00112600
P	1.79198900	-0.24386400	-0.11717900

Atom	x	y	z
H	2.19424500	0.51697300	1.00794900
H	1.67992400	-1.46192400	0.61321500

Coordinates [Å] for the optimized geometry of **1b**.

Atom	x	y	z
N	-1.83582000	-0.78807800	-0.04024000
H	-1.66328600	-1.35328100	0.78352600
H	-1.54583600	-1.28674100	-0.87523900
N	-1.21936300	0.44758800	0.05501100
H	-1.82424500	1.25697800	0.01918700
C	0.12334900	0.68563300	0.01542600
O	0.59003000	1.80494800	-0.01196100
P	1.18434300	-0.87699900	-0.10318000
H	2.34710000	-0.21251800	0.35215400
H	0.84706500	-1.41941200	1.16779000

Coordinates [Å] for the optimized geometry of **TS**.

Atom	x	y	z
N	-1.82007000	-0.84198100	-0.30318900
H	-1.11621800	-1.50229300	-0.63896500
H	-2.21252100	-0.36840800	-1.10946600
N	-1.27133900	0.15557800	0.54127600
H	-1.21658500	-0.22217000	1.48242200
C	0.01577500	0.62856100	0.09900000
O	0.19402500	1.76593800	-0.23857800
P	1.38629300	-0.67022400	-0.09844000
H	2.44252000	0.23209500	0.16472000
H	1.30142400	-1.17991700	1.22590400
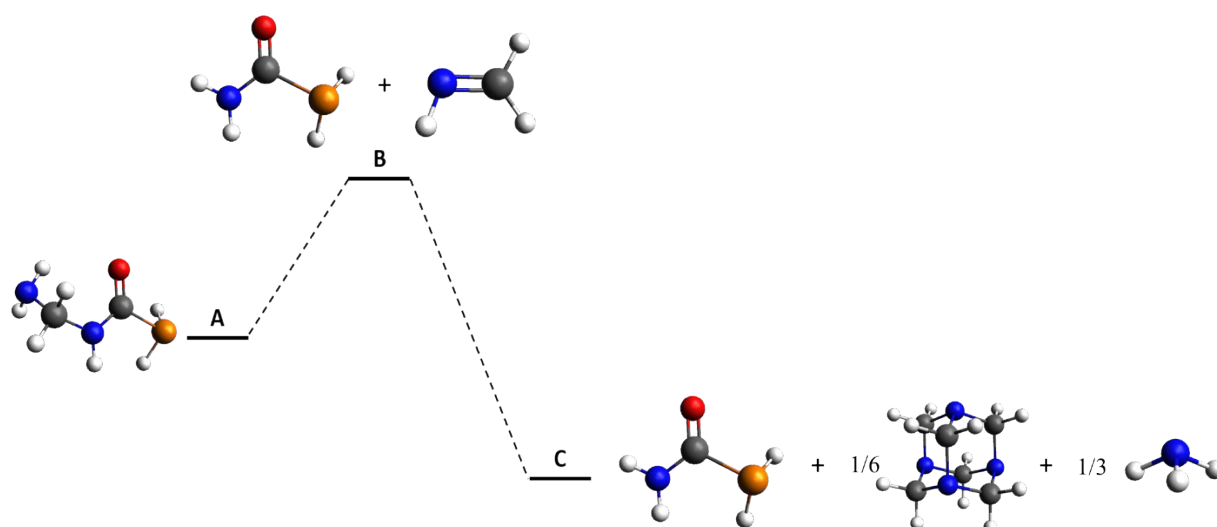
Figure S36: Schematic representation of the energy of the two proposed stages of decomposition of the methylenediamine mono-phosphinecarboxamide derivative. ΔG is given in kJ mol–1: A = 0; B = 45; C = –8.

Table S11: Calculated total bonding energies of the proposed decomposition products of the methylenediamine mono-phosphinecarboxamide derivative (**A**) given in kJ mol⁻1, with ΔG relative to the most stable isomer of **A** given in brackets.

	A	**B**		**C**		
	trans-A	$H_2NC(O)PH_2$	$HNCH_2$	$H_2NC(O)PH_2$	Urotropine	NH_3
Individual Energy	−1591042.0	−1342896.3	−248100.2	−1342896.3	−1192394.6	−148263.4
Total Energy	−1591042.0 (0)	−1590996.5 (45)		−1591049.9 (−8)		

Coordinates [Å] for the optimized geometry of ***trans*-A**.

Atom	x	y	z
C	-0.431722	0.249563	-0.136361
O	-0.110631	1.414505	-0.305053
P	-2.248025	-0.206759	0.058332
H	-2.080000	-1.308907	0.945533
H	-2.477958	0.730369	1.095109

Atom	x	y	z
N	0.457632	-0.772048	-0.181070
H	0.158829	-1.705539	0.050907
C	1.876623	-0.501928	-0.439960
H	2.351336	-1.471482	-0.615292
H	1.934605	0.077217	-1.365478
N	2.592100	0.215103	0.575795
H	2.175818	1.134614	0.679271
H	2.525255	-0.258120	1.470238

Coordinates [Å] for the optimized geometry of **$H_2NC(O)PH_2$**.

Atom	x	y	z
C	0.526131	0.152344	0.008789
O	1.019087	1.261556	0.007188
P	-1.342062	-0.059393	-0.119606
H	-1.469756	-1.215847	0.702803
H	-1.612507	0.850119	0.931022
N	1.257053	-0.991638	-0.006336
H	2.261877	-0.906019	0.011507
H	0.842466	-1.902407	0.082878

Coordinates [Å] for the optimized geometry of **$HNCH_2$**.

Atom	x	y	z
N	-0.668752	-0.153678	0.000022
H	-1.156331	0.745882	-0.000069
C	0.584596	0.028468	-0.000037
H	1.088210	1.004530	0.000107
H	1.241811	-0.845470	0.000030

Coordinates [Å] for the optimized geometry of **Urotropine**.

Atom	x	y	z
N	0.479292	1.319247	-0.516206
C	0.069839	0.438434	-1.613957
N	-0.407468	-0.866629	-1.148387
C	0.672302	-1.486588	-0.375135
N	1.100938	-0.666839	0.761745
C	1.531629	0.632609	0.238276
C	-0.672771	1.486692	0.374343
C	-1.531752	-0.632880	-0.237461
C	-0.069466	-0.438262	1.613916
N	-1.172608	0.214247	0.902929
H	0.923895	0.285872	-2.284621
H	-0.729688	0.927383	-2.183136
H	0.330091	-2.459409	-0.002617
H	1.531406	-1.655078	-1.035366
H	2.398407	0.483054	-0.416364
H	1.840849	1.268931	1.076089
H	-0.383588	2.130992	1.213063
H	-1.479450	1.983423	-0.177810
H	-1.892625	-1.598506	0.136309
H	-2.346546	-0.154562	-0.793941
H	0.226017	0.189165	2.463229
H	-0.418537	-1.401479	2.004707

Coordinates [Å] for the optimized geometry of **NH₃**.

Atom	x	y	z
N	0.000000	0.000000	0.117810
H	0.000000	0.935955	-0.274889
H	-0.810561	-0.467977	-0.274889
H	0.810561	-0.467977	-0.274899
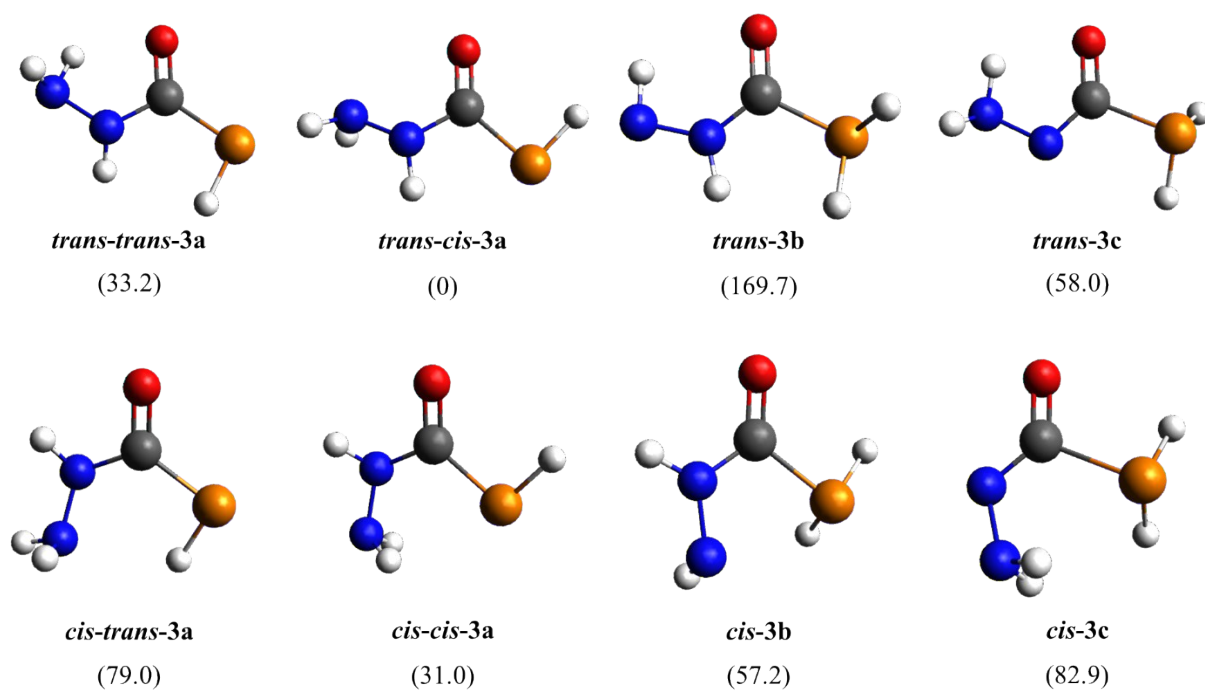
Figure S37: Possible deprotonation isomers of **3** relative to the C–N and C–P bonds. The calculated relative ΔG values are given in brackets in kJ mol⁻¹.

Coordinates [Å] for the optimized geometry of *trans-trans*-**3a**.

Atom	x	y	z
N	2.207392	-0.381475	0.149188
N	0.870153	-0.765410	-0.147783
C	-0.092000	0.286088	-0.047837
P	-1.838551	-0.162087	0.027997
O	0.355050	1.445194	-0.021419
H	2.093565	0.584493	0.484703
H	2.658600	-0.254003	-0.756523
H	0.598983	-1.570660	0.399397
H	-1.604109	-1.578405	-0.098992

Coordinates [Å] for the optimized geometry of *trans-cis*-**3a**.

Atom	x	y	z
C	-0.116375	0.380986	-0.089687
O	0.150026	1.580334	-0.016157
P	-1.715633	-0.473741	0.073057
H	-2.476160	0.732925	0.082054
N	0.932215	-0.558959	-0.345783
H	0.607132	-1.505947	-0.169634
N	2.197320	-0.265306	0.186625
H	2.285003	-0.573864	1.153904
H	2.909818	-0.705724	-0.380698

Coordinates [Å] for the optimized geometry of *trans*-**3b**.

Atom	x	y	z
C	-0.066339	0.326968	0.041397
P	1.702645	-0.275335	-0.123586
H	2.199677	0.228797	1.124174
H	1.601768	-1.615567	0.380163
O	-0.264976	1.563039	0.003614
N	-1.007156	-0.622448	0.012278
H	-0.684443	-1.576800	0.080387
N	-2.371544	-0.502857	0.007384
H	-2.487927	0.504614	-0.145862

Coordinates [Å] for the optimized geometry of *trans*-**3c**.

Atom	x	y	z
C	0.084904	0.235255	0.021482
O	0.334208	1.468654	-0.006288
P	-1.740508	-0.244963	-0.129274
H	-1.763950	-1.469662	0.601324
H	-2.224818	0.521465	0.973984
N	0.879110	-0.806700	0.049587
N	2.257672	-0.381585	0.105635
H	2.706118	-0.841901	-0.686498
H	2.249699	0.621780	-0.114838

Coordinates [Å] for the optimized geometry of *cis-trans*-**3a**.

Atom	x	y	z
P	1.388811	-0.806636	0.002926
H	0.432940	-1.831915	-0.279542
O	0.542014	1.762021	0.103479
C	0.230349	0.568840	-0.044568
N	-1.177762	0.389924	-0.264078
H	-1.603943	1.223736	0.142208
N	-1.790459	-0.824944	0.087069
H	-1.886141	-0.917193	1.099256
H	-2.715682	-0.839155	-0.327183

Coordinates [Å] for the optimized geometry of *cis-cis*-**3a**.

Atom	x	y	z
N	1.183875	0.483311	0.185259
N	1.820564	-0.736455	-0.121401
C	-0.221131	0.618300	0.034019
O	-0.647300	1.774380	-0.061246
P	-1.116947	-0.970065	0.023828
H	1.656524	1.278876	-0.227395
H	-2.381092	-0.329238	-0.154157
H	1.247877	-1.203176	-0.836278
H	1.705005	-1.328322	0.699262

Coordinates [Å] for the optimized geometry of *cis*-**3b**.

Atom	x	y	z
C	-0.135851	0.710174	0.031793
O	-0.708285	1.809145	-0.006762
P	-0.967107	-0.978431	-0.109092
H	-0.604734	-1.570334	1.130431
H	-2.221457	-0.467505	0.402462
N	1.181687	0.487859	0.066497
H	1.772086	1.311797	-0.036288
N	1.675302	-0.804899	-0.171518
H	2.043172	-1.112408	0.738255

Coordinates [Å] for the optimized geometry of *cis*-**3c**.

Atom	x	y	z
C	-0.042650	-0.766555	0.015265
O	0.584199	-1.826645	-0.004105
P	1.141077	0.876019	-0.107655
H	0.815128	1.577878	1.095674
H	2.236399	0.186083	0.477900
N	-1.337972	-0.551867	0.042344
N	-1.776085	0.799269	-0.054941
H	-1.573005	1.279990	0.826700
H	-1.213967	1.296437	-0.756017

4. References

[1] D. Heift, Z. Benkő and H. Grützmacher, *Dalton Trans.* 2014, **43**, 831–840.

[2] M. J. Frisch, G. W. Trucks, H. B. Schlegel, G. E. Scuseria, M. A. Robb, J. R. Cheeseman, G. Scalmani, V. Barone, G. A. Petersson, H. Nakatsuji, X. Li, M. Caricato, A. Marenich, J. Bloino, B. G. Janesko, R. Gomperts, B. Mennucci, H. P. S.I.54 Hratchian, J. V. Ortiz, A. F.

Izmaylov, J. L. Sonnenberg, D. Williams-Young, F. Ding, F. Lipparini, F. Egidi, J. Goings, B. Peng, A. Petrone, T. Henderson, D. Ranasinghe, V. G. Zakrzewski, J. Gao, N. Rega, G. Zheng, W. Liang, M. Hada, M. Ehara, K. Toyota, R. Fukuda, J. Hasegawa, M. Ishida, T. Nakajima, Y. Honda, O. Kitao, H. Nakai, T. Vreven, K. Throssell, J. A. Montgomery, Jr., J. E. Peralta, F. Ogliaro, M. Bearpark, J. J. Heyd, E. Brothers, K. N. Kudin, V. N. Staroverov, T. Keith, R. Kobayashi, J. Normand, K. Raghavachari, A. Rendell, J. C. Burant, S. S. Iyengar, J. Tomasi, M. Cossi, J. M. Millam, M. Klene, C. Adamo, R. Cammi, J. W. Ochterski, R. L. Martin, K. Morokuma, O. Farkas, J. B. Foresman, and D. J. Fox, *Gaussian 09, Revision D.01,* Gaussian, Inc., Wallingford CT, **2016**.

[3] J. P. Perdew, K. Burke and M. Ernzerhof, *Phys. Rev. Lett.* 1996, **77**, 3865–3868.

[4] W. J. Hehre, R. Ditchfield and J. A. Pople, *J. Chem. Phys.* 1972, **56**, 2257–2261; P. C. Hariharan and J. A. Pople, *Theoret. Chim. Acta*, 1973, **28**, 213–222; M. M. Franci, W. J. Pietro, W. J. Hehre, J. S. Binkley, M. S. Gordon, D. J. DeFrees and J. A. Pople, *J. Chem. Phys.*, 1982, **77**, 3654–3665.